SANDIA REPORT
SAND88—2338 • UC—35
Unlimited Release
Printed October 1988

Explosive Shaped Charge Penetration Into Tuff Rock

M. G. Vigil

Prepared by
Sandia National Laboratories
Albuquerque, New Mexico 87185 and Livermore, California 94550
for the United States Department of Energy
under Contract DE-AC04-76DP00789

SF2900Q(8-81)

Issued by Sandia National Laboratories, operated for the United States Department of Energy by Sandia Corporation.

Printed in the United States of America
Available from
National Technical Information Service
U.S. Department of Commerce
5285 Port Royal Road
Springfield, VA 22161

NTIS price codes
Printed copy: A04
Microfiche copy: A01

SAND88-2338 UC-35
Unlimited Release

Printed October 1988

EXPLOSIVE SHAPED CHARGE PENETRATION INTO TUFF ROCK

Manuel G. Vigil

Explosive Subsystems Division
Sandia National Laboratories
Albuquerque, NM 87185-5800

ABSTRACT

Analysis and data for the use of Explosive Shaped Charges (ESC) to generate holes in tuff rock formation is presented. The ESCs evaluated include Conical Shaped Charges (CSC) and Explosive Formed Projectiles (EFP). The CSCs vary in size from 0.158 to 9.1 inches inside cone diameter. The EFPs were 5.0 inches in diameter. Data for projectile impact angles of 30 and 90 degrees are presented. Analytically predicted depth of penetration data generally compared favorably with experimental data. Predicted depth of penetration versus ESC standoff data and hole profile dimensions in tuff are also presented.

ACKNOWLEDGMENTS

The author wishes to thank those persons who contributed to this study, namely, Donnie Marchi, 2512, for fabrication of test setup hardware, obtaining all test measurements, and involvement in conducting the tests. Duane Smith, 7173, and Dave Kessel, 7173, coordinated the scheduling, setup of safety procedures and arming and firing for these tests.

TABLE OF CONTENTS

TABLES

FIGURES

Figures cont'd

EXPLOSIVE SHAPED CHARGE PENETRATION INTO TUFF ROCK

I. Introduction

Explosive Shaped Charges (ESC) were used to generate holes in tuff rock formations. This ESC technology has application in the mining industry[1], road construction, demolition, excavation, petroleum industry and general rock barrier penetration work. Several Conical Shaped Charges (CSC) and one Explosive Formed Projectile (EFP) were evaluated. The CSCs vary in size from 0.158 to 9.1 inches inside cone diameter. The EFPs were 5.0 inches in diameter. ESC generated hole profiles in tuff are presented. Analytically predicted ESC depth of penetration data are compared to experimental data. Predicted CSC penetration versus standoff data are included.

The general ESC -- tuff target configuration for this study is shown in Figure 1. The general explosive shaped charge configurations considered for this study are shown in Figure 2.

The three ESCs shown in Figure 2 produce three different projectiles as illustrated in Figures 3 - 5 for a conical shaped charge (CSC), hemispherical shaped charge (HSC) and explosive formed projectile (EFP), respectively. For any homogeneous target material that will flow under high dynamic pressure impact conditions, a CSC will produce the smallest diameter and deepest hole. The EFP will produce the largest diameter and shallowest hole in the target. The HSC should produce a hole profile where diameter and depth of penetration are between the CSC and EFP limits. Only CSCs and EFPs were used in this study.

After each test, a small diameter hollow tube, with a high pressure air hose attached, was inserted into the hole to blow out or clean the hole as shown in Figure 6. A measuring tape as shown in Figure 7 or a solid, steel rod about 0.375 inches in diameter, as shown in Figure 8, were used to measure the hole depth. An inclinometer along with the steel rod were used to measure the hole angle (α) relative to the target surface. Different diameter, wooden spheres on threaded aluminum rods were used to measure the hole diameter at a given depth. Other methods for measuring hole profile proved to be too expensive.

II. Development

Tuff Rock Formation

The ESC tests were conducted in the welded tuff formations at Tonopah Test Range in Nevada. The density of the tuff is 1.85 grams per cubic centimeter and the unconfined compression strength is 23 megapascals or 3338 pounds per square inch. The porosity of the tuff is about 5 percent.

Conical Shaped Charges

A detailed historical background for the development of conical shaped charge (CSC) technology is presented in Reference 1. A brief summary of major historical CSC events is listed in Table I and References 2 -- 19. Reference 19 lists 99 references on the theory and operation of conical shaped charges. General configurations for CSCs are shown in Figure 9 -- 10. Figure 9 illustrates the large number (20) of variables involved in the design of a CSC. An optimized CSC cross-section is illustrated in Figure 11. It is assumed that the reader has some knowledge of the functioning[19] of CSCs.

The cross-sections for the CSCs evaluated in this study are shown in Figures 12 -- 17. Figures 12 and 13 show the cross-section and steel housing for the 0.158 inch diameter CSC, respectively. Figures 14 -- 17 illustrate the configurations for 3.86, 4.66, 6.986, and 9.125 inch inside diameter CSCs.

The ESC liner inside diameter, liner material, apex angle, explosive type, explosive weight and tamping material are listed in Table II. The eleven ESC tests conducted in this study are listed in Table III. The first nine tests involved CSCs.

Radiographs for the 0.158 inch diameter CSC jet are shown in Figure 18 at one microsecond intervals. The jet diameter aft of the tip is about 0.025 inches and the jet length just before breakup is about 0.5 inches. The measured jet tip velocity is 5.5 millimeter per microsecond. Figures 19 and 20 show radiographs of the 9.125 inch diameter CSC (M3) jet. Three flash X-ray heads were used to expose the two films shown in Figures 19 and 20. The three jet paths indicated on the radiographs are a result of each of the three different X-ray heads projecting the jet profile onto three different heights on the film. The jet had not arrived along the top path in Figure 19 film which was located down stream of the film of Figure 20 relative to the jet tip. The jet diameter aft of the tip is about 0.70 inches and the jet length before breakup is about 30 inches. The measured jet tip velocity was 7.1 millimeters per microsecond.

Predicted CSC Jet Penetration

The Shaped Charge Analysis Program (SCAP)[20,21] code developed at Sandia National Laboratories was used to predict the CSC jet penetrations in Tuff. This code uses a hydrodynamic model for target penetration. The model works well for targets that flow hydrodynamically under high dynamic pressure loading conditions. It was assumed that the tuff rock material would flow like metallic target materials. Figures 21 -- 25 show the SCAP code predictions of jet penetration versus standoff for the 0.158, 3.86, 4.66, 6.986, and 9.125 inch diameter CSCs, respectively. The SCAP code predicted and measured jet penetration versus CSC cone inside diameter data are compared in Figure 26.

CSC Test Results

CSC tests were conducted at 30 (shallow impact) and 90 (normal impact) degrees relative to the tuff target surface as illustrated in Figure 27. The standoffs were varied as shown in Table III. The 3.86 and 4.66 inch diameter CSC tests were conducted with relatively short (7 inch) and with relatively long (27 and 36 inches, respectively) standoffs.

Figures 28, 30, 32, and 34 show the test configuration for the 3.86, 4.66, 7.0, and 9.125 inch diameter CSCs. Figures 29, 31, 33, and 35 show the CSC generated holes in the tuff rock for the above CSCs, respectively. All CSC tests shown are for 90 degree orientations of the CSC relative to the tuff surface. The measured CSC standoff (S.O.), jet penetration (P), entrance hole diameter (D_e), hole bottom diameter (D_b), surface crater depth (H_c) and hole center line to target surface angle (α) data are listed in Table III for all tests.

The target entrance hole diameter (D_e) as a function of CSC diameter is shown in Figure 36 for CSCs with copper liners. The bottom of the hole diameter versus CSC diameter is shown in Figure 37 for CSCs with copper liners.

Explosive Formed Projectile

The dimensions for the EFP[22] used in this study are shown in Figure 38. The EFP explosive, copper liner, and tamping (casing) parameters are listed in Table IV. The EFP slug or projectile parameters are listed in Table V. The upper liner is shown in Figure 39. The EFP projectile penetration into rolled homogeneous armor (RHA) versus standoff is shown in Figure 40.

Predicted EFP Slug Penetration

The only simple predictive tool for projectile penetration is the following modified Bernoulli equation:[23]

$$1/2\ \rho_p(V_p - U)^2 + Y_p = 1/2\ \rho_t U^2 + R_t$$

where,
U = projectile penetration velocity
Y_p = projectile strength factor
R_t = target strength factor
ρ_t = target density
ρ_p = projectile density
V_p = projectile velocity

The SCAP code cannot model EFPs. Hydrodynamic codes would require equation of state parameters for the tuff material which are not readily known. Modeling the collapse of the EFP disk could present some difficulties in addition to the expense.

Since the strength factors (Y_p, R_t) for the tuff and copper were not known, these terms were dropped in the above equation resulting in the familiar square root density law[19] for high velocity impact:

$$P = L(\rho_p/\rho_t)^{0.5}$$

The above equation was used to estimate the EFP penetration (P) in the tuff target:

where,
L = 10.0 inches (Table V) = projectile length
ρ_p = 8.96 g/cc
ρ_t = 1.85 g/cc

Thus,

$$P = 22.1 \text{ inches}$$

A second similar method was also used. Since the EFP slug penetration in steel (RHA)[22] is known, and shown in Figure 40, then for the same EFP, the following relationship can be derived:

$$(P_{TUFF}/P_{Steel}) = (\rho_{Steel}/\rho_{TUFF})^{0.5}$$

from Figure 40,
at Standoff = 12 inches
P_{Steel} = 9.2 inches
ρ_{Steel} = 7.86 g/cc

$$P_{TUFF} = 19 \text{ inches}$$

The above two methods predict EFP slug penetrations into tuff of 19 -- 22.1 inches. The square root density law relationship for projectile (slug) penetration to slug length ratio as a function of square root of projectile density for various target materials including tuff is shown in Figure 41.

The EFP slug velocity was calculated using the Taylor Piston model[24] for barrel tamped flyers:

$$V_s = DA[(Z-1)/(Z+1)]$$

where,

V_s	= maximum slug velocity = 3.4 mm/microsecond
A	= $[8/(G^2-1)]^{0.5}$ = 1.0
Z	= $[1 + (32\, C_e/27M)]^{0.5}$ = 2.24
D	= detonation velocity = 8.8 mm/microsecond
G	= explosive detonation product gas exponent = 3.0
C_e	= discounted or effective explosive
weight	= C(ALPHA) = 945g (Ref. 24)
ALPHA	= explosive discount factor = 0.35
M	= liner weight = 280g
C	= actual explosive weight = 2700g

The calculated EFP slug velocity was 3.4 millimeters per microsecond which agrees well with the measured values of 3.83 (slug tip) to 2.4 (slug tail) millimeters per microsecond (average velocity = 3.1).[22]

EFP Test Results

EFP tests were conducted at 30 and 90 degrees relative to the tuff target surface as illustrated in Figure 27. The standoffs were varied as shown in Table III.

Figures 42 and 44 show the test configurations for 90 and 30 degree impacts, respectively. Figures 43 and 45 show the EFP slug generated holes in the tuff rock. The measured EFP standoff (S.O.), slug penetration (P), entrance hole diameter (D_e), bottom of the hole diameter (D_b), surface crater depth (H_c) and hole centerline to target surface angle (α) data are listed in Table III for both tests.

III. Summary

Conical shaped charges (CSC) and explosive formed projectiles (EFP) have been shown to be useful in generating holes in tuff rock. CSCs varying in diameter from 0.158 to 9.125 inches and an EFP of 5.0 inch diameter were used to generate holes in tuff with parameters in the following ranges (for 90 degree impacts and excluding the 0.158 inch CSC):

Penetration depth:	23.5 - 55 inches
Entrance hole diameter:	1.2 - 5.5 inches
Bottom of hole diameter:	0.5 - 2 inches
Surface crater diameter:	6 - 23 inches
Depth of surface crater:	1 - 8 inches

The CSCs generated the maximum depth of penetration with the 4.66 inch diameter CSC producing a 55 inch hole in the Tuff. The EFP generated the largest diameters with 5.5 inches at the entrance and 2.0 inches at the bottom.

The SCAP code predictions of CSC jet penetration in tuff versus standoff were generally in good agreement with the experimental data, as illustrated in Table VI. The simple hydrodynamic square root density law relationship for EFP slug penetration predictions were in reasonable agreement with the experimental data. Therefore, hydrodynamic theory describes the CSC jet and EFP slug penetration in tuff reasonably well.

IV. References

1. C. F. Austin, Lined - Cavity Shaped Charges and Their Use in Rock and Earth Materials, New Mexico Institute of Mining & Technology, Bulletin 69, 1959.

2. C. E. Munroe, Modern Explosives, Scribners Mag., v. 3, p. 563-576, 1888.

3. C. E. Munroe, The Application of Explosives, Pop. Sci. Monthly, v. 56, p. 444-455, 1900.

4. R. W. Wood, Optical and Physical Effects of High Explosives, Roy. Soc. Proc., v. 157, p. 249-260, 1936.

5. F. A. Korolev and G. I. Pokrovskii, Investigation of the Jet Action of Explosives by an Optical Method, Doklady Akad. Nauk. (U.S.S.R.), v.42, p. 266-267, 1944.

6. V. Torrey, Bazooka's Grandfather, Pop. Sci. Monthly, v. 146, p. 65-69, 211-216, 1945.

7. V. Torrey, Shaped Charge, Munroe Effect, Explosives Eng., v. 23, p. 160-163, 1945.

8. J. B. Huttl, The Shaped Charge for Cheaper Mine Blasting, Eng. Min. J., v. 147, p. 58-63, 1946.

9. R. S. Lewis and G. B. Clark, Application of Shaped Explosive Charges to Mining Operations: Tests on STeel and Rock, Univ. of Utah Bull. 5, p. 1-37, 1946.

10. H. C. Draper, J. E. Hill, and W.. G. Agnew, Shaped Charges Applied to Mining, Part I, Drilling HOles for Blasting, U. S. Bur. Mines Rpt. Inv. 4371, 1948.

11. G. Birkhoff, D. P. MacDougall, E. M. Pugh, and G. Taylor, Explosives with Lined Cavities, J. Appl. Phys., v. 19, p. 563-582, 1948.

12. L. S. Byers, The Multiple Jet Shaped Blasting Charge--Why it Functions, Pit and Quarry, v. 41, p. 98-102, 1949.

13. L. S. Byers, New Plurajet Shaped Blasting Charges Ready for Industry, Pit and Quarry, v. 42, p. 79-81, 1950.

14. J. T. Gardiner, Use of Shaped Charge Process for Open Hole Shooting, World Oil, v. 131, p. 99-103, 1950.

15. M. P. Lebourg and G. R. Hodgson, A method of Perforating Casing Below Tubing, Am. Inst. Min. Met. Eng., Pet. Br., Trans., v. 195, p. 303-310, 1952.

16. M. P. Lebourg and W. T. Bell, Perforating of Multiple Tubingless Completions, Am. Inst. Min. Met. Eng., Soc. Pet. Eng., 34th annual fall meeting, Paper 1298-G, 1959.

17. V. C. Davis, Taconite Fragmentation, U. S. Bur. Mines Prt. Inv. 4918, 1953.

18. R. M. Hyatt, Bazooka at Work, Pop. Mech., v. 112, p. 115-117, 208, 1959.

19 P. C. Chou and W. J. Flis, Recent Developments in Shaped Charge Technology, Propellants, Explosive, Pyrotechnics, 11, 99-114, 1986.

20. M. G. Vigil, Optimized Conical Shaped Charge Design Using the SCAP Code, SAND88-1790, Sandia National Laboratories, Albuquerque, NM, August 1988.

21. A. C. Robinson SCAP-A Shaped Charge Analysis Program - User's Manual for SCAP 1.0, SAND85-0708, Sandia National Laboratories, Albuquerque, NM, April 1985.

22. Design and Fabrication of EFP Assemblies, Final Report, Dyna East Corporation, Report No. DE-TC-87-01, February 17, 1987.

23. A. Tate, Long Rod Penetration Models - Part II. Extensions to the Hydrodynamic Theory of Penetration, Int. J. Mech. Sci. Vol. 28, No. 9, pp. 599-612, 1986.

24. R. A. Benham, Analysis of the Motion of a Barrell-Tamped Explosively Propelled Plate, SAND 78-1127, Sandia National Laboratories, September 1978.

Table I. Historical Background for Conical Shaped Charges (CSC)

Year	Person	Discovery	Reference
1888	Charles E. Monroe	Unlined cavity effect	2,3
1910	Egon Neumann	Unlined cavity effect	--
1936	R. W. Wood	Lined cavity/high velocity jet	4
1944	Korolev & Pokrovski	High velocity copper jet (No. 8 blasting cap)	5
1945	Voltra Torrsy	First unclassified publications on military CSCs	6,7
1946	J. B. Huttl	First publication on CSC use in mining	8
1947	Lewis, Clark, Brunckner	Additional publications on CSC use in mining	9
1948	H. C. Draper, J. E. Hill W. G. Agnew	CSCs applied to mining, drilling holes for blasting	10
1948	Birkoff, MacDougal, Prigh, Taylor	First paper on jet formation and penetration theory	11
1949	L. S. Byers	CSC marketed for mining	12,13
1950	J. T. Gardiner	CSC use in Petroleum industry	14
1952	M. P. Lebourg, G. R. Hodgson	CSC use in Petroleum industry	15,16
1953	V. C. Davis	Publication on CSC for mining	17
1959	R. M. Hyatt	Bazooka at work	18
1986	P. C. Chou, W. J. Flis	Recent development in CSC technology	19

Table II. Explosive Shaped Charge Parameters

Type	Diameter	Liner Material	Apex Angle (deg)	Explosive	Explosive Weight (lb)	Tamping Material
CSC	0.158	Copper	47	LX-13	0.002	Steel
CSC	3.860	Copper	42	Octol	3.500	Aluminum
CSC	4.660	Copper	60	Octol	5.330	Aluminum
CSC	6.986	Glass	60	Comp B	9.500	Fiberglass
CSC	9.125	Steel	60	Comp B	30.000	Steel
EFP	5.000	Copper	--	LX-14	5.95	Steel

Table III. Shaped Charge/Tuff Penetration Tests at Tonopah

Test No.	Shaped Charge	D Dia.	S.O. (in)	P Depth (in)	Hole Profile D_e (in)	D_b (in)	D_c (in)	H_c (in)	α (deg)
1	CSC	0.15	0.16	0.92	0.12	0.07	0.84	0.13	90
2	CSC	3.86	24	27.0[1]	1.20	?	10.0	7.5	90
3	CSC	3.86	7	37.5	3.0	7.0[2]	8.5	2.8	87
4	CSC	3.86	24	43.0	1.13	0.5	29.0	6.0	31
5	CSC	4.66	36	53.0	1.50	0.5	9.0	8.0	90
6	CSC	4.66	7	55.0	3.5	16.4[2]	6.0	1.0	89
7	CSC	4.66	36	52.5	1.50	0.5	35.0	7.0	28
8	M2A3/CSC	7.0	14	46.0	3.50	44.0[2]	14.5	4.0	88
9	M3/CSC	9.13	20	50.0	5.50	40.0[2]	23.0	4.0	89
10	JTI/EFP	5.0	12	23.5	5.50	23.0[2]	14.0	3.0	90
11	JTI/EFP	5.0	12	13.5	7.00[3]		40.0	6.5	30

D = shaped charge diameter
S.O. = standoff
P = penetrating depth
D_e = hole entrance diameter
D_b = hole bottom diameter
CSC = conical shaped charge
EFP = explosively formed projectile
NA = not applicable
α = impact angle
D_c = surface crater diameter
H_c = surface crater depth

(1) = unable to clean hole out with air compressor
(2) = Depth for 2 inch diameter ball
(3) = EFP projectile ricochet

Table IV. EFP Parameters

Explosive[22]

Lx-14
2.7 Kg (5.95 lb)
ρ = 1.83 g/cc
Detonation velocity = 8.8 mm/microsecond

Copper Liner[22]

Weight = 280 grams

Casing/Tamping[22]

Stainless Steel
Weight = 3357.2 g

Table V. Explosive Formed Projectile Slug Parameters

Slug Parameters[22]		Value
1.	Diameter	0.75 inches
2.	Length	10.0 inches
3.	Tip Velocity	3.83 mm/microsecond
4.	Tail Velocity	2.4 mm/microsecond
5.	Mass	280 grams
6.	Energy	1.35 megajouls
7.	Breakup Time	255 microseconds at 43.3 inches

Table VI. Predicted CSC Jet Penetration In Tuff

CSC Diameter	Impact Angle (deg).	Standoff (in)		Penetration (in)		
		Measured	SCAP	Measured	SCAP	% Diff.
0.158	90	0.2	0.2	0.92	1.2	30
3.860	90	24	24	27.0*	51	--
3.860	30	7	7	43.0	47	10
4.660	90	36	36	53.0	54	4
4.660	30	7	7	52.5	49	7
6.986	90	14	14	46.0	54	17
9.125	90	20	20	50.0	43	13

* = Unable to clean hole

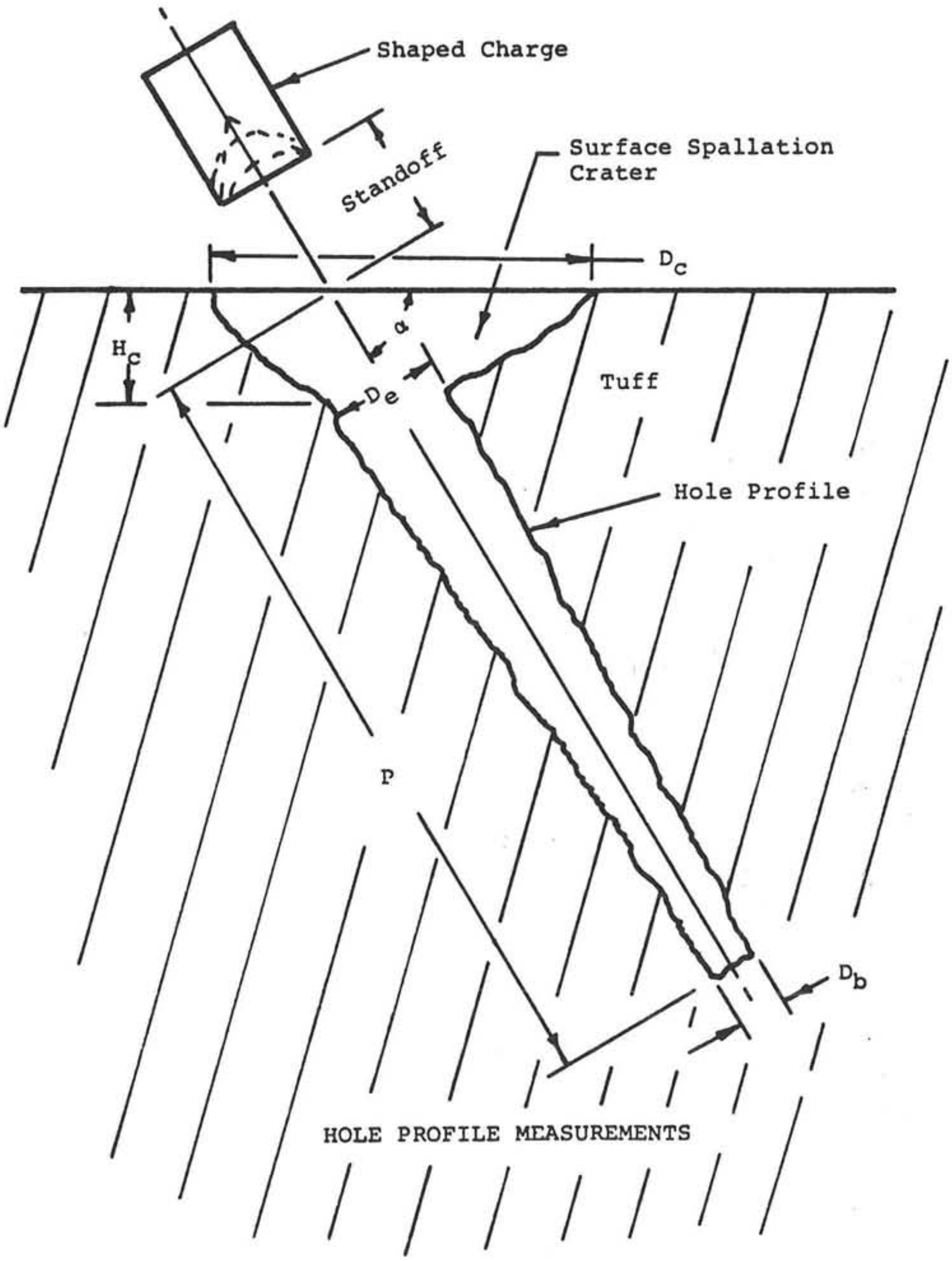

Figure 1. General Explosive Shaped Charge
Tuff Target Configuration

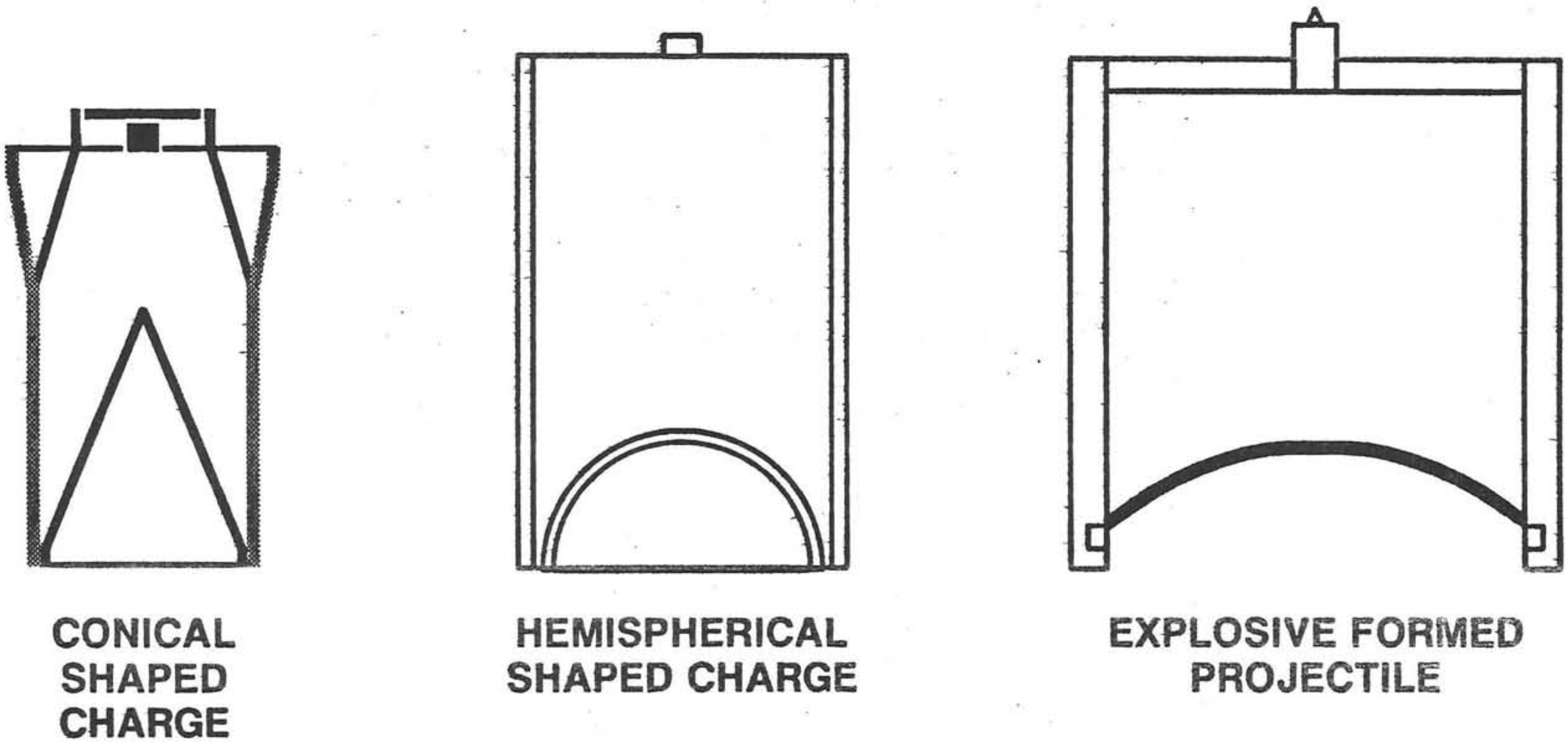

Figure 2. General Explosive Shaped Charge Configurations

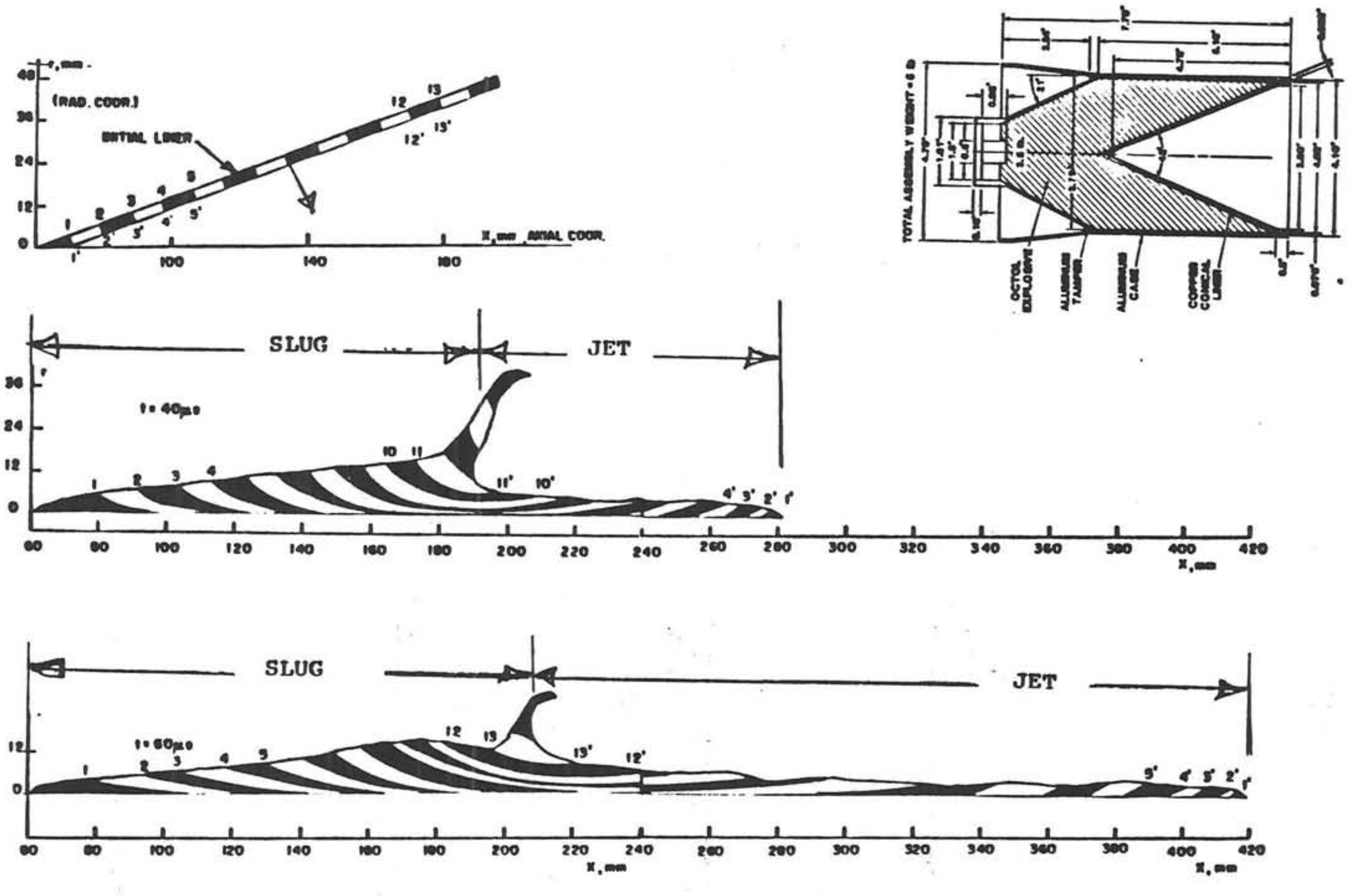

Figure 3. Hydrocode Simulation of an 42° Conical Shaped Charge, Initial Liner Configuration, and Jet Slug Formation at 40 and 60 μs

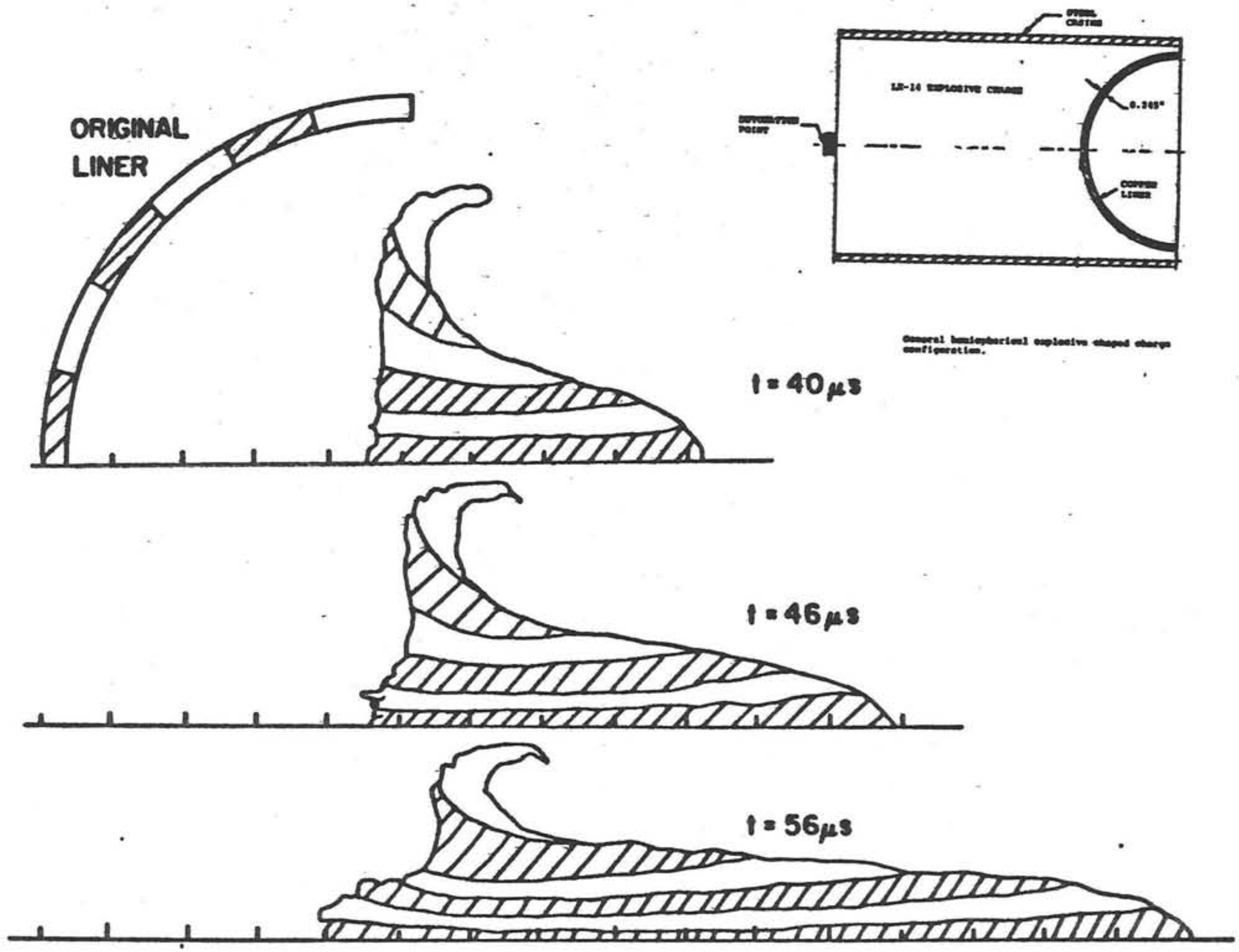

Figure 4. Hydrocode Simulation of Jet Formation From A Hemispherical Shaped Charge For The Point-Initiated Case at Three Times After Detonation

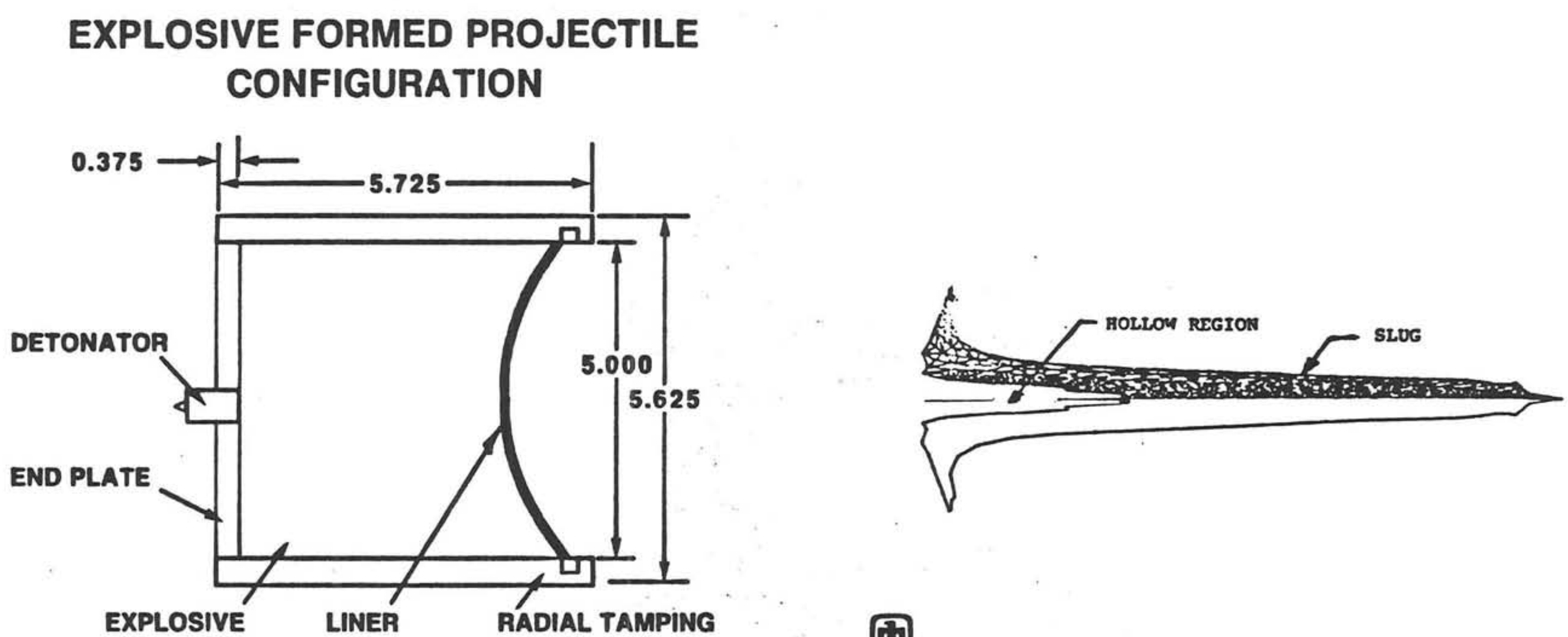

Figure 5. Slug Shape for 5 Inch-Diameter EFP at 200 μs After Detonation

Figure 6. Steel, Hollow Tube With High Pressure Hose Attached For Cleaning Holes in Tuff Formation

Figure 7. Steel Tape Used to Measure Hole Depth

Figure 8. Solid Steel Rod Used to Measure Hole Depth

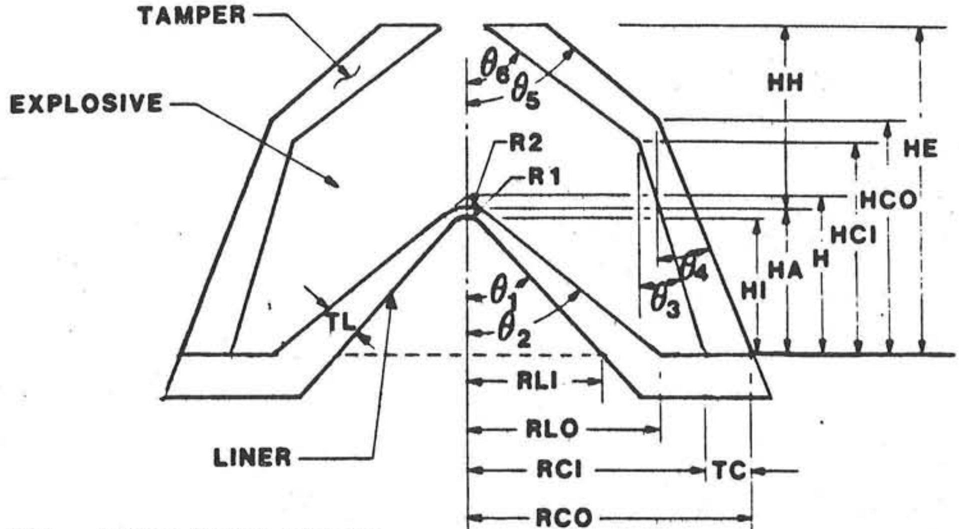

RLI - LINER INNER RADIUS
RLO - LINER OUTER RADIUS
RCI - CONFINEMENT/SHEATH INNER RADIUS
RCO - CONFINEMENT/SHEATH OUTER RADIUS
HI - LINER INNER HEIGHT
HA - LINER ACTUAL HEIGHT
H - LINER THEORETICAL APEX HEIGHT
HCI - CONFINEMENT/SHEATH INNER HEIGHT
HCO - CONFINEMENT/SHEATH OUTER HEIGHT
HE - EXPLOSIVE HEIGHT
HH - EXPLOSIVE HEIGHT ABOVE APEX
TL - LINER THICKNESS
TC - CONFINEMENT/SHEATH THICKNESS
R1 - LINER INNER APEX RADIUS
R2 - LINER OUTER APEX RADIUS
θ_1 - LINER INNER APEX HALF ANGLE
θ_2 - LINER OUTER APEX HALF ANGLE
θ_3 - CONFINEMENT/SHEATH INNER APEX HALF ANGLE
θ_4 - CONFINEMENT/SHEATH OUTER APEX HALF ANGLE

Figure 9. General Conical Shaped Charge Cross-Section Parameters

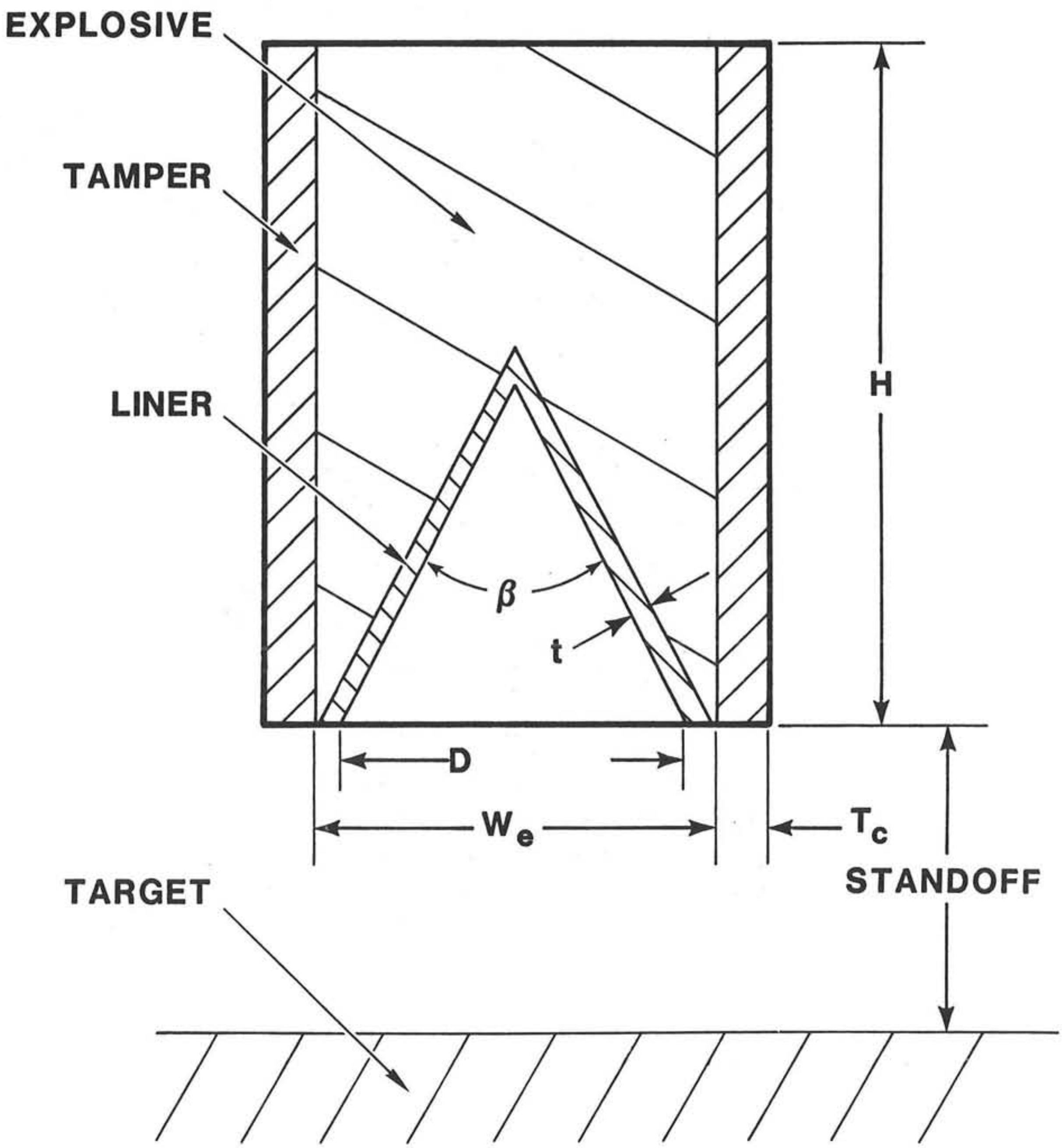

Figure 10. Basic Conical Shaped Charge Cross-Section

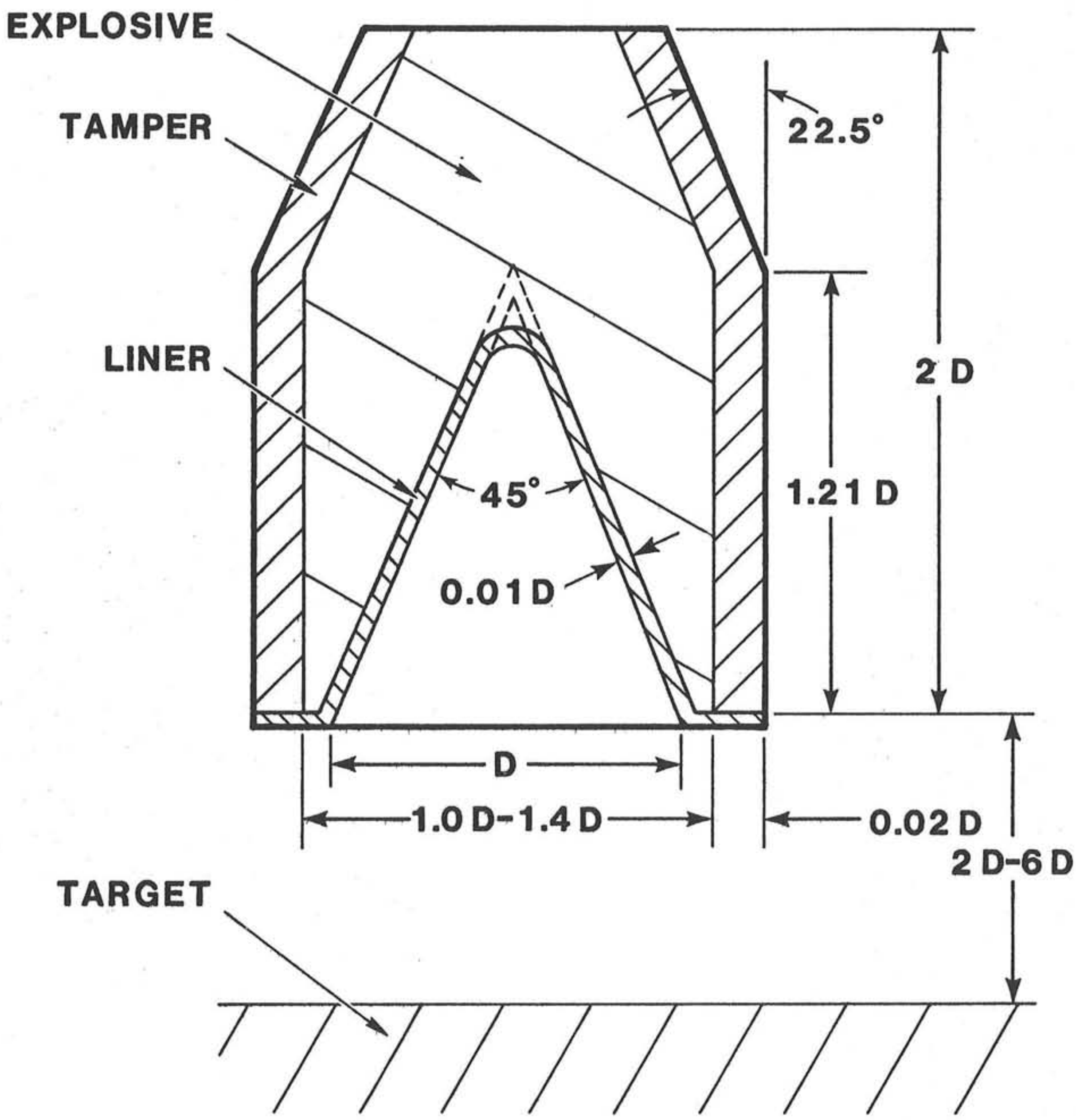

Figure 11. Optimized Conical Shaped Charge Configuration

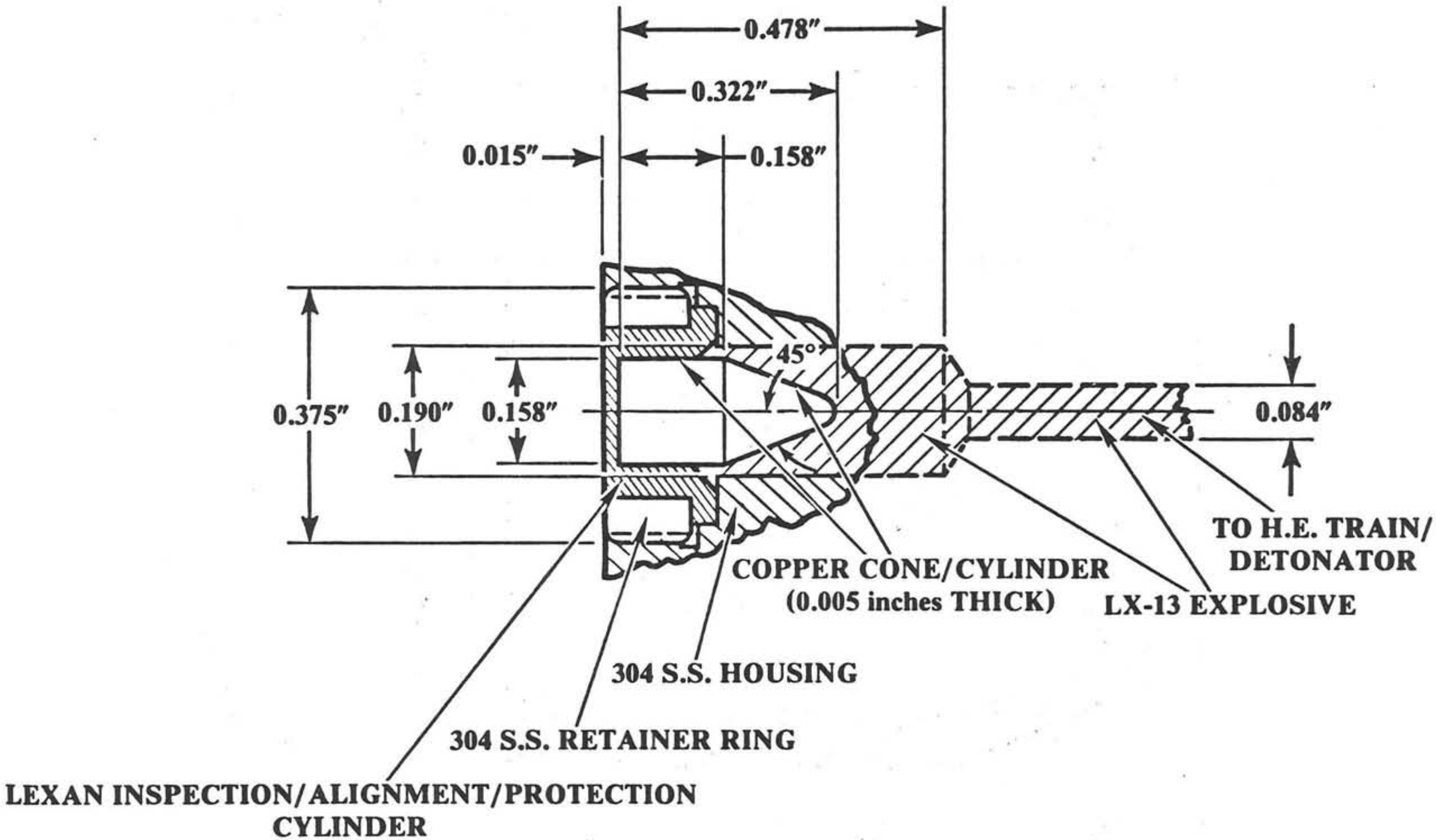

Figure 12. Conical Shaped Charge Configuration

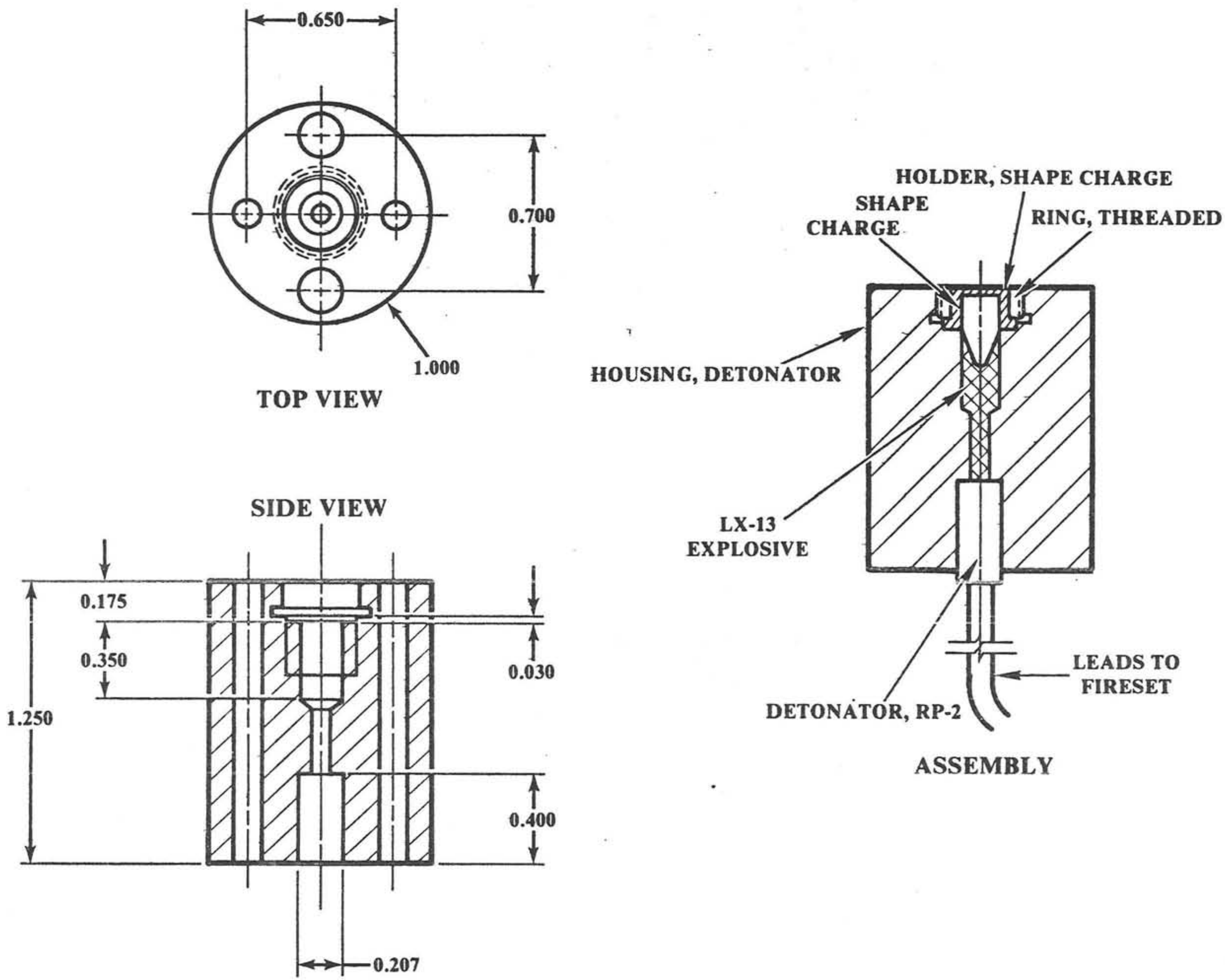

Figure 13. CSC Development Test Housing Configurations

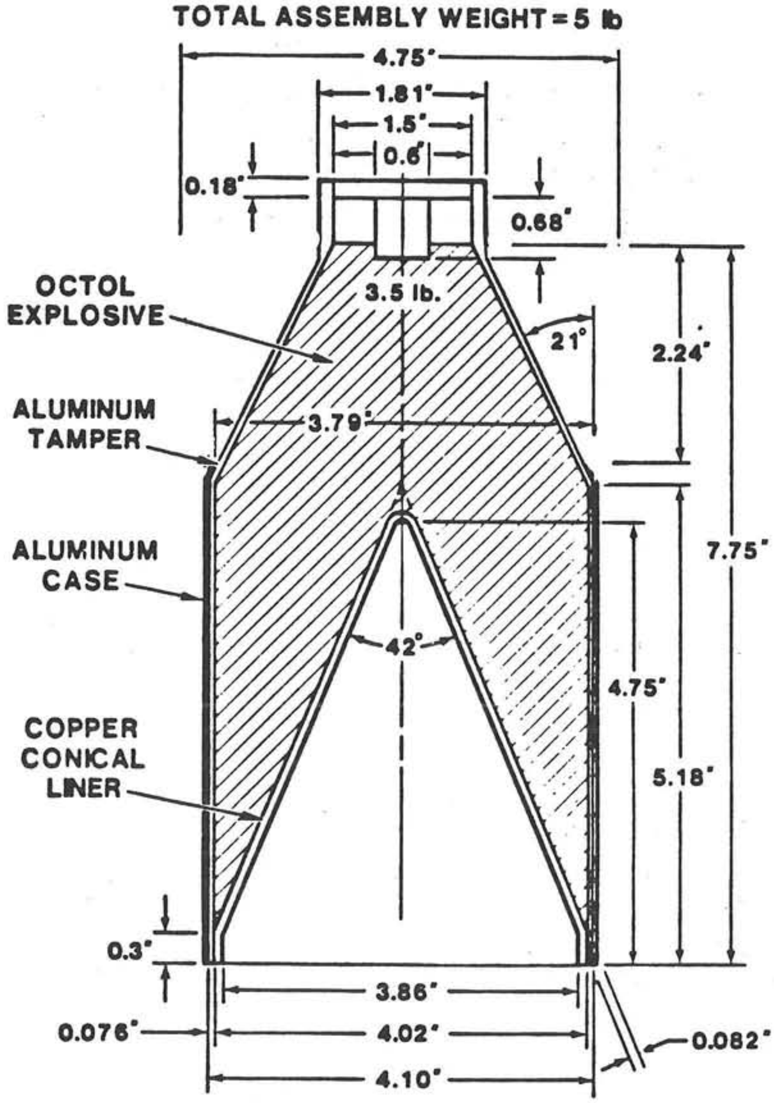

Figure 14. 3.86 Inch Diameter CSC Cross-Section

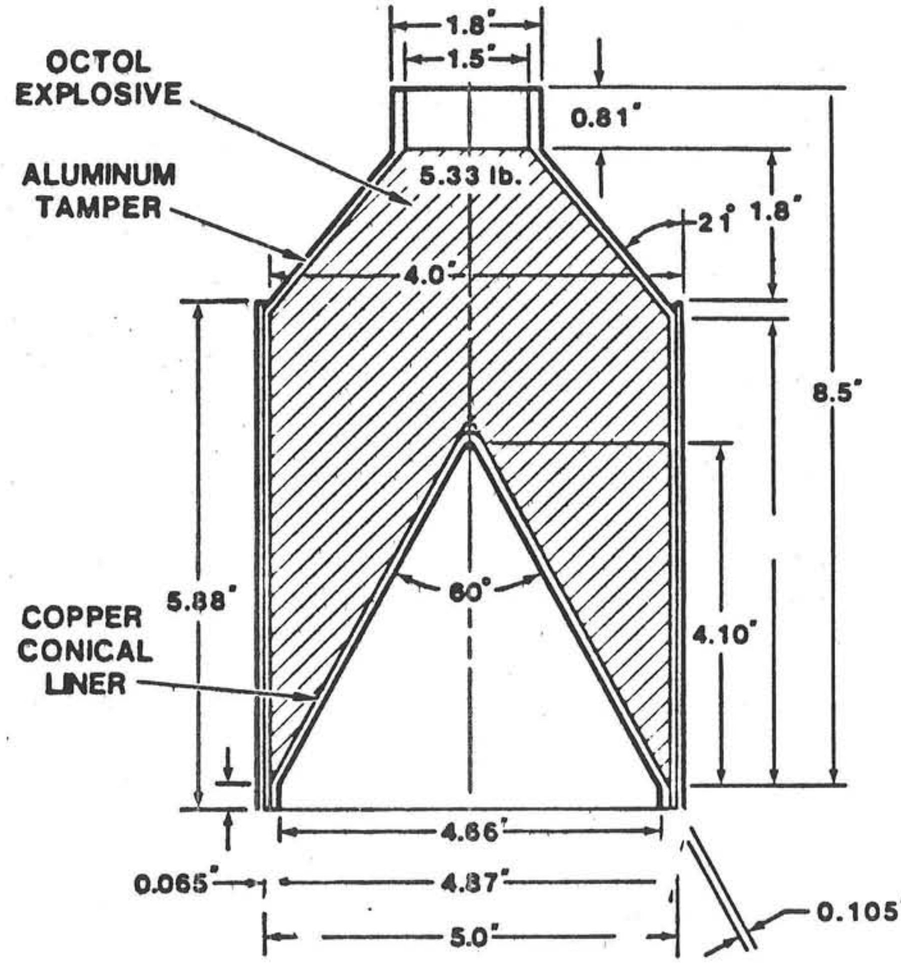

Figure 15. 4.66 Inch Diameter CSC Cross-Section

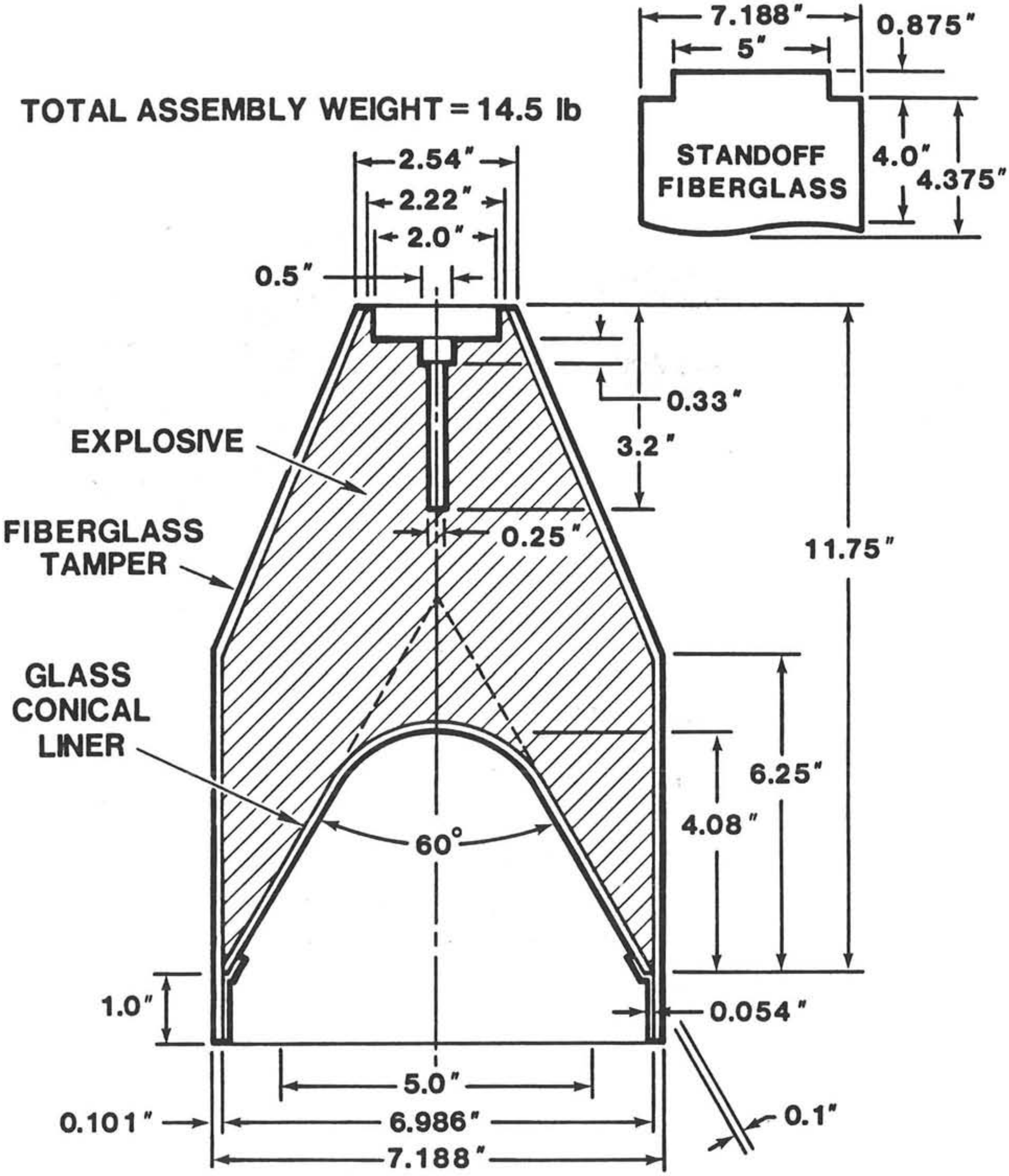

Figure 16. M2A3 Conical Shaped Charge Configuration

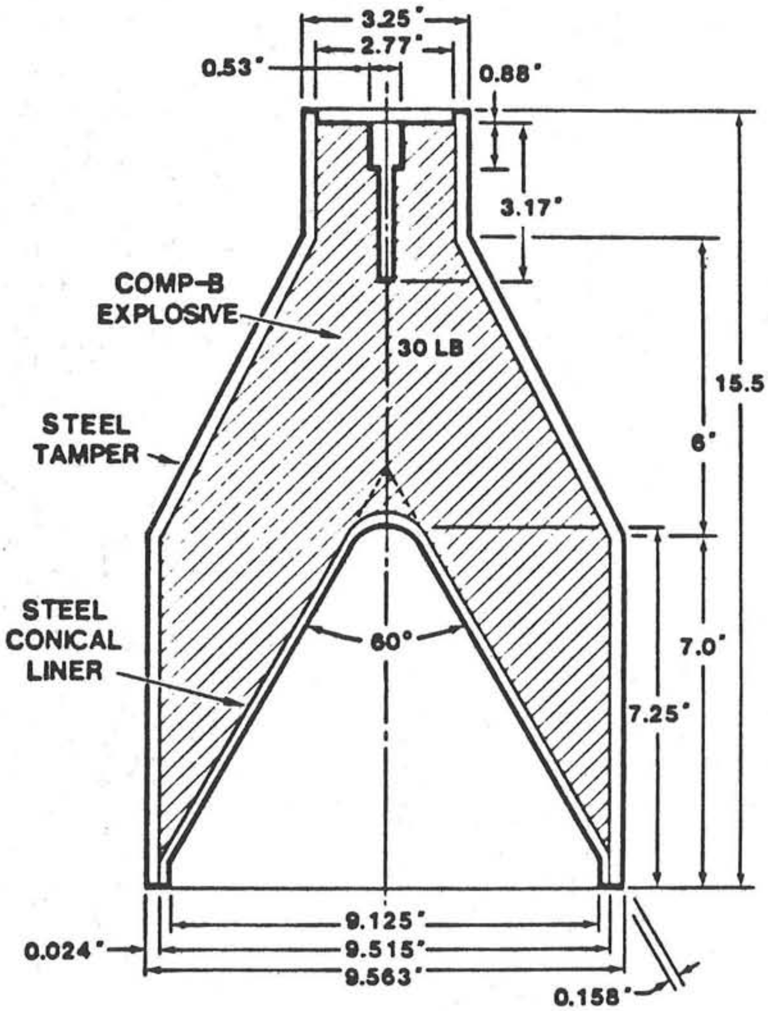

Figure 17. M3 9.125 Inch Diameter CSC Cross-Section

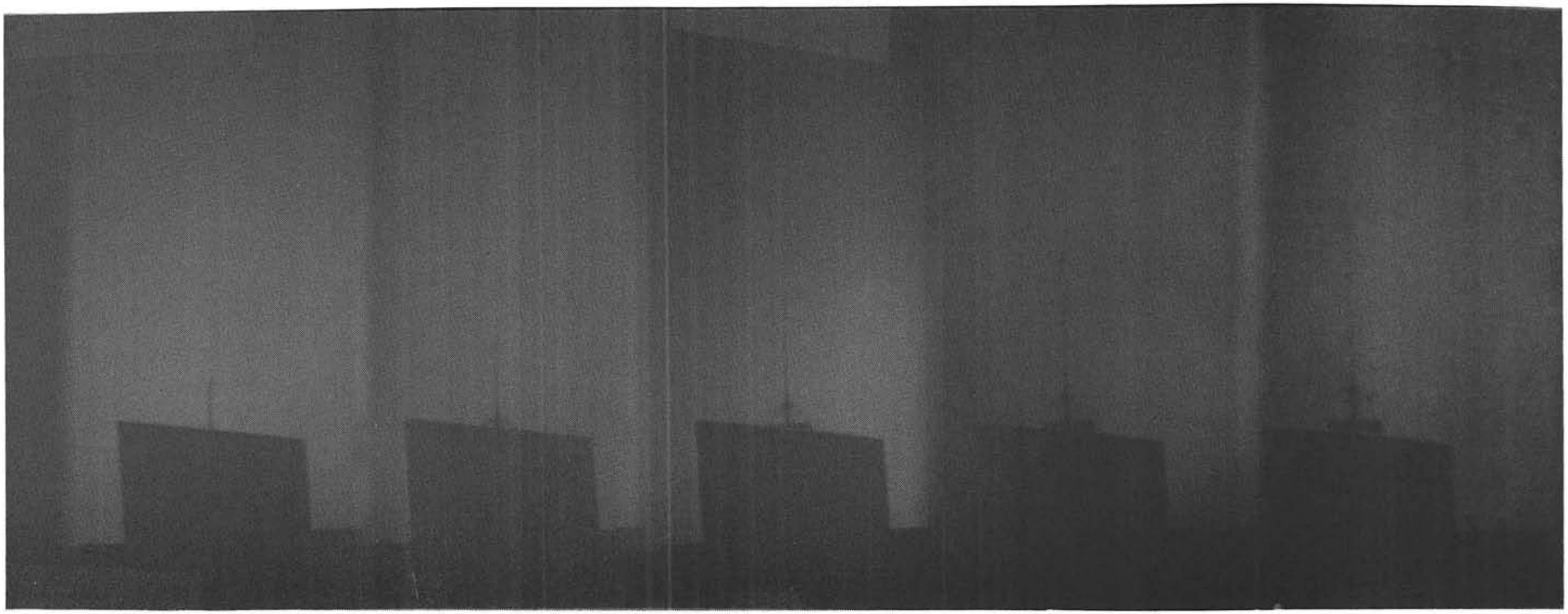

Figure 18. Conical Shaped Charge Copper Jet (Liner/I.D. - 0.158", Apex Angle = 45°, Thickness =- 0.005", Stamped)

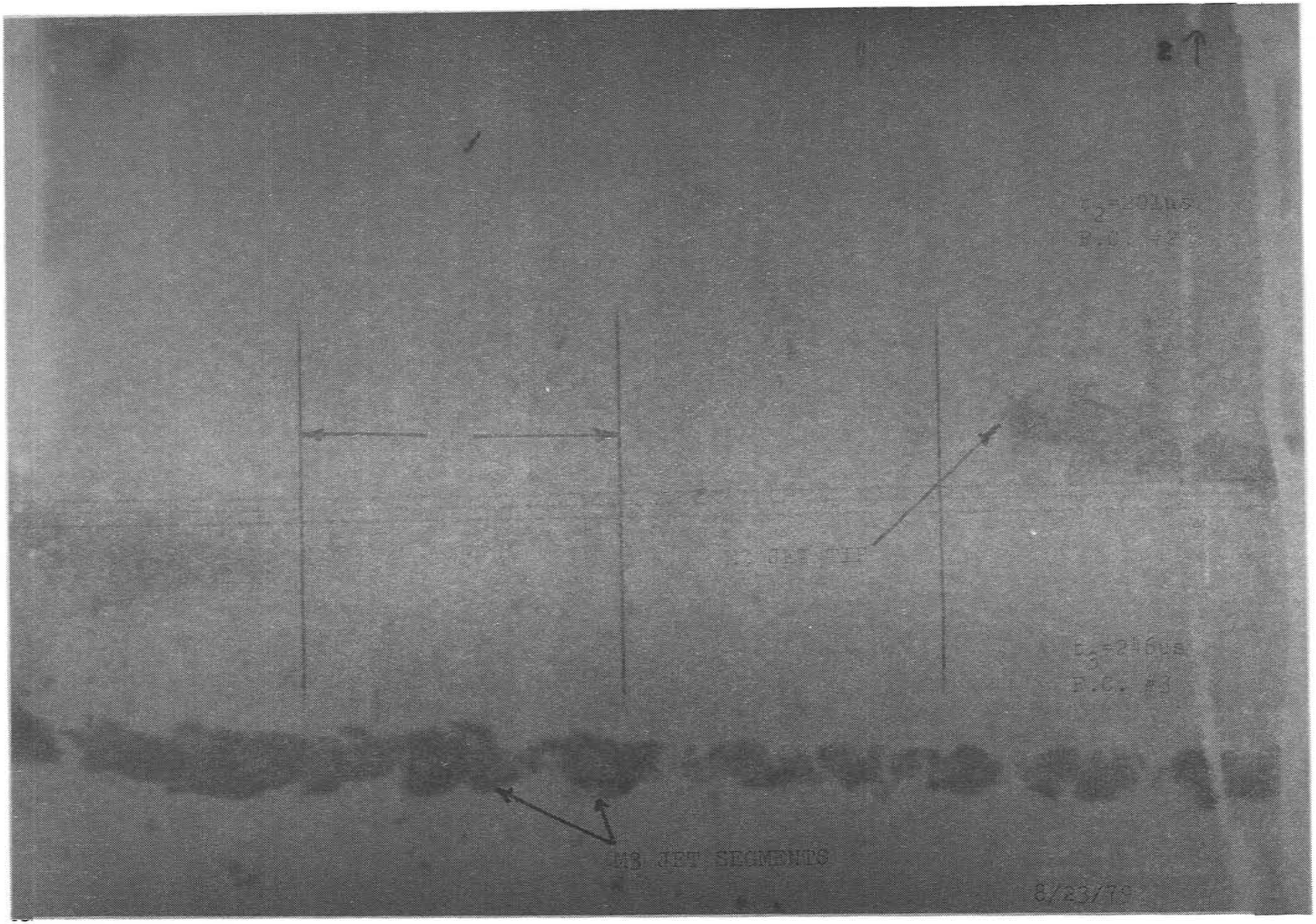

Figure 19. Film Cassette #2 Showing Jet Tip at 201 μs from Detonation

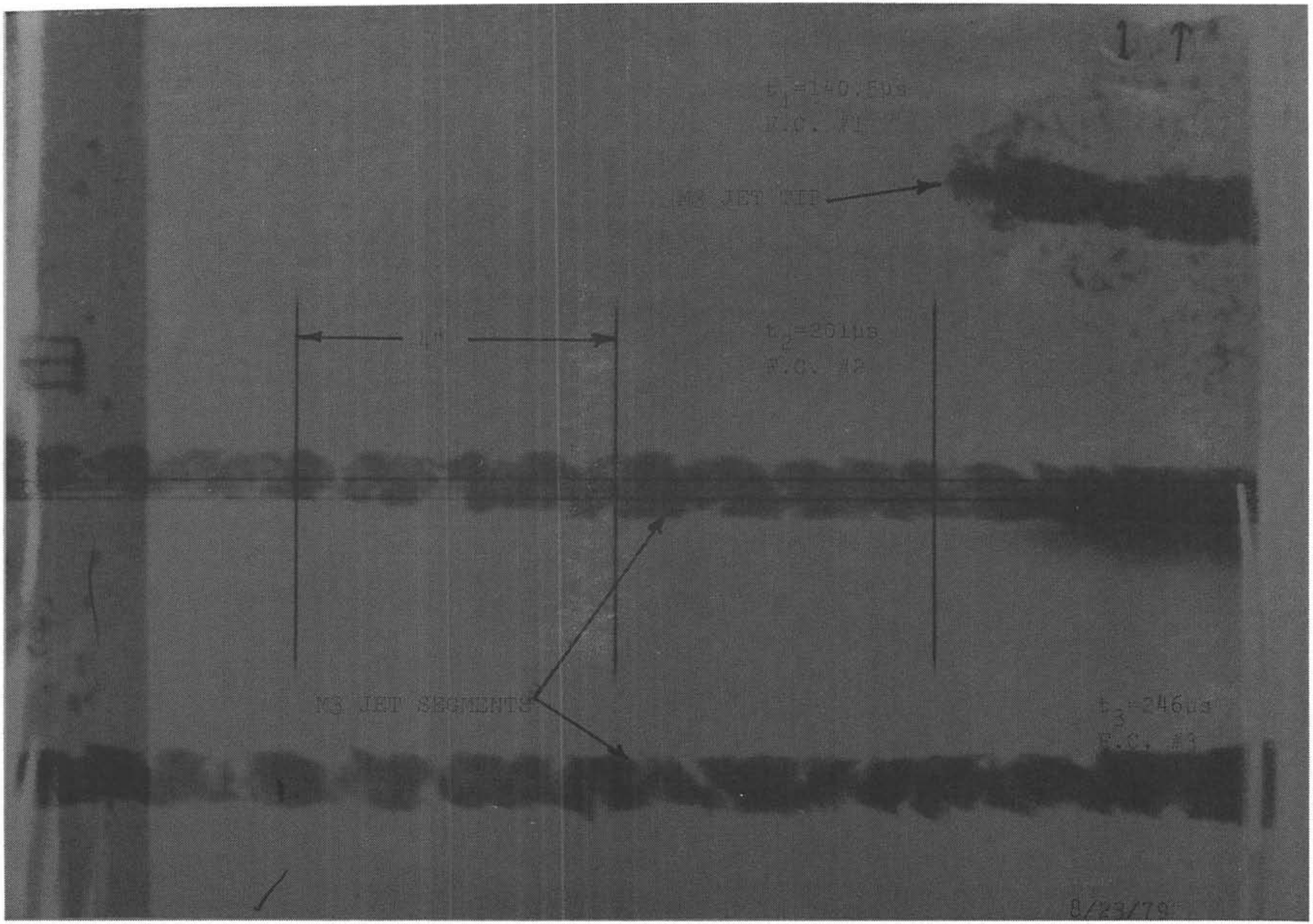

Figure 20. Flash X-Ray Triple Exposure of Cassette #1
Showing Jet Tip At 140.5 μs

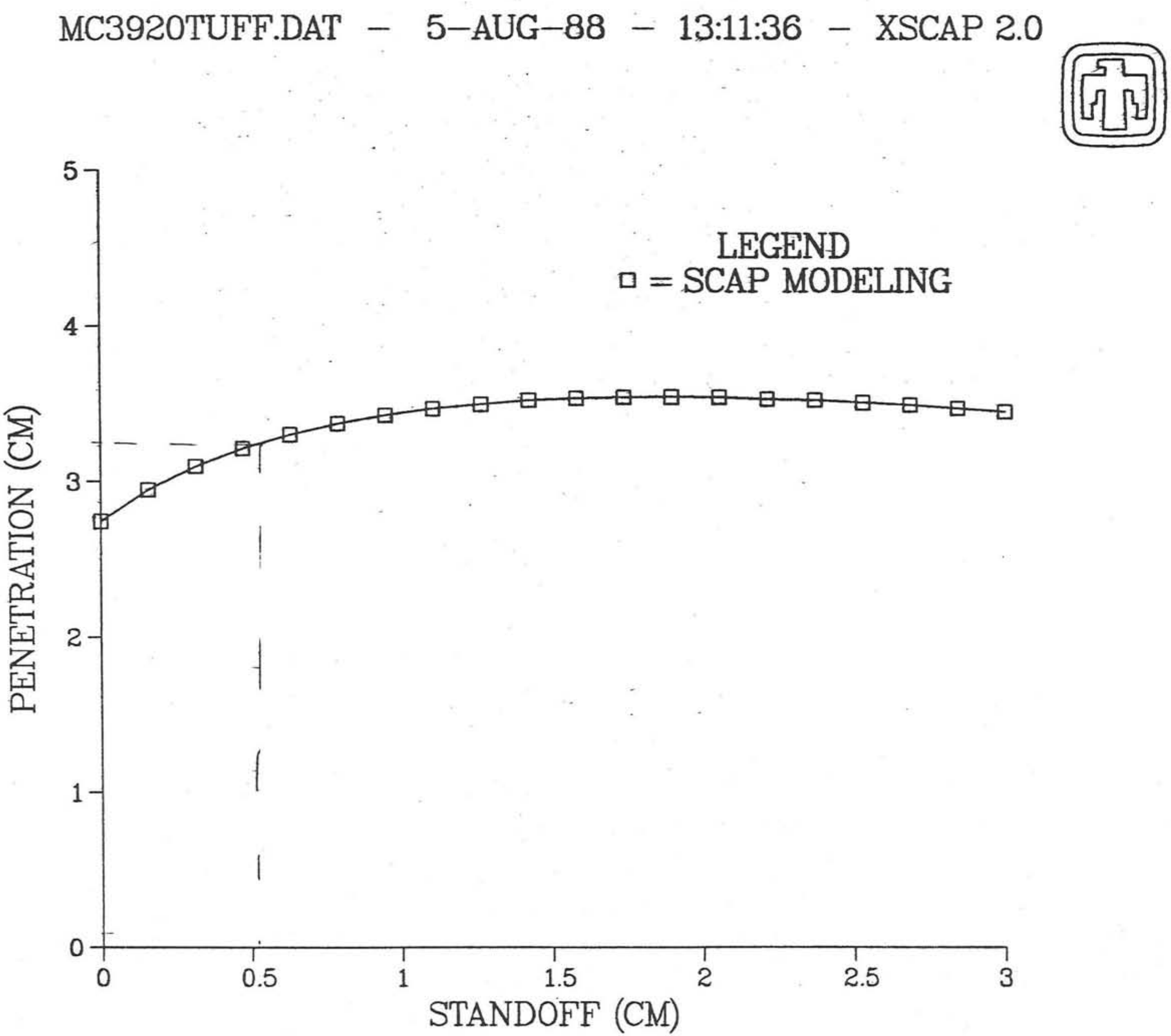

Figure 21. 0.158 Inch Diameter CSC Penetration Versus Standoff

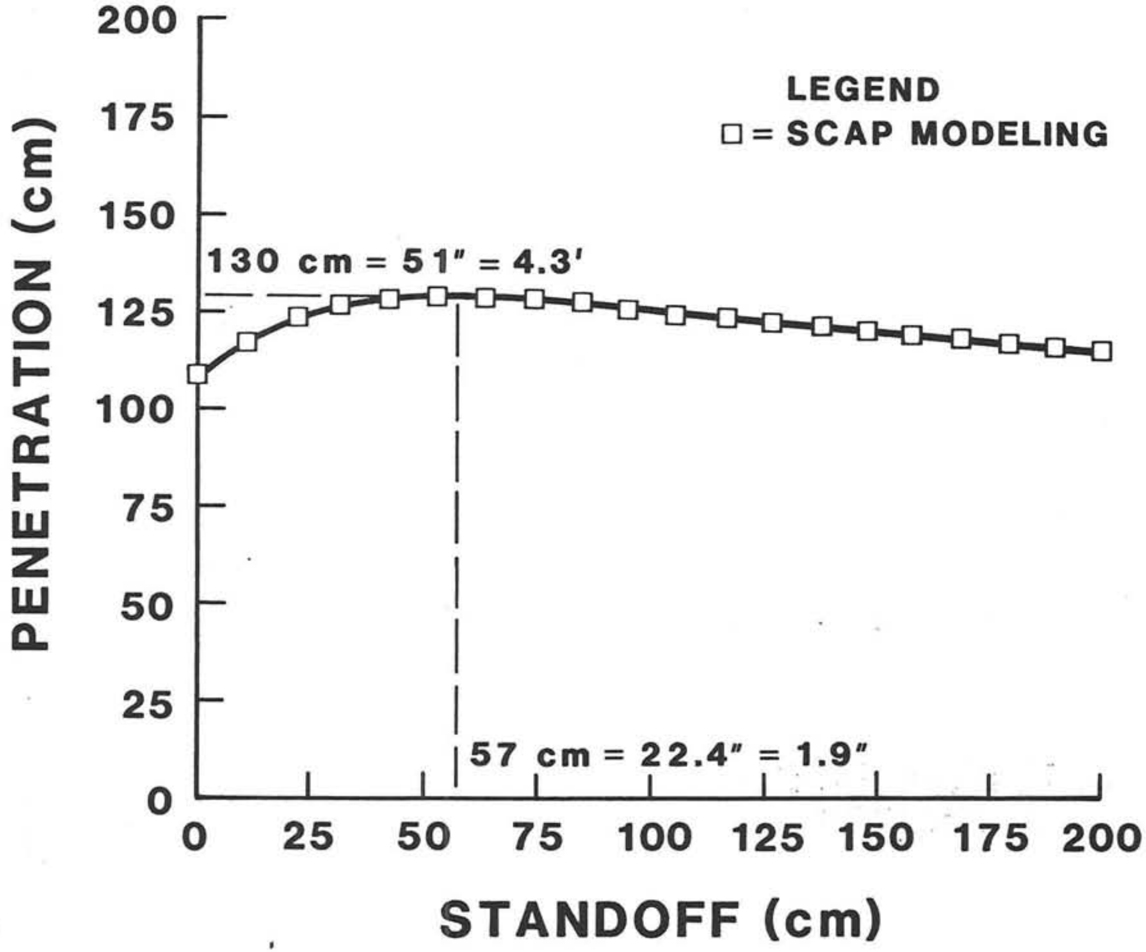

Figure 22. 3.86 CSC Jet Penetration Versus Standoff for a Tuff Target

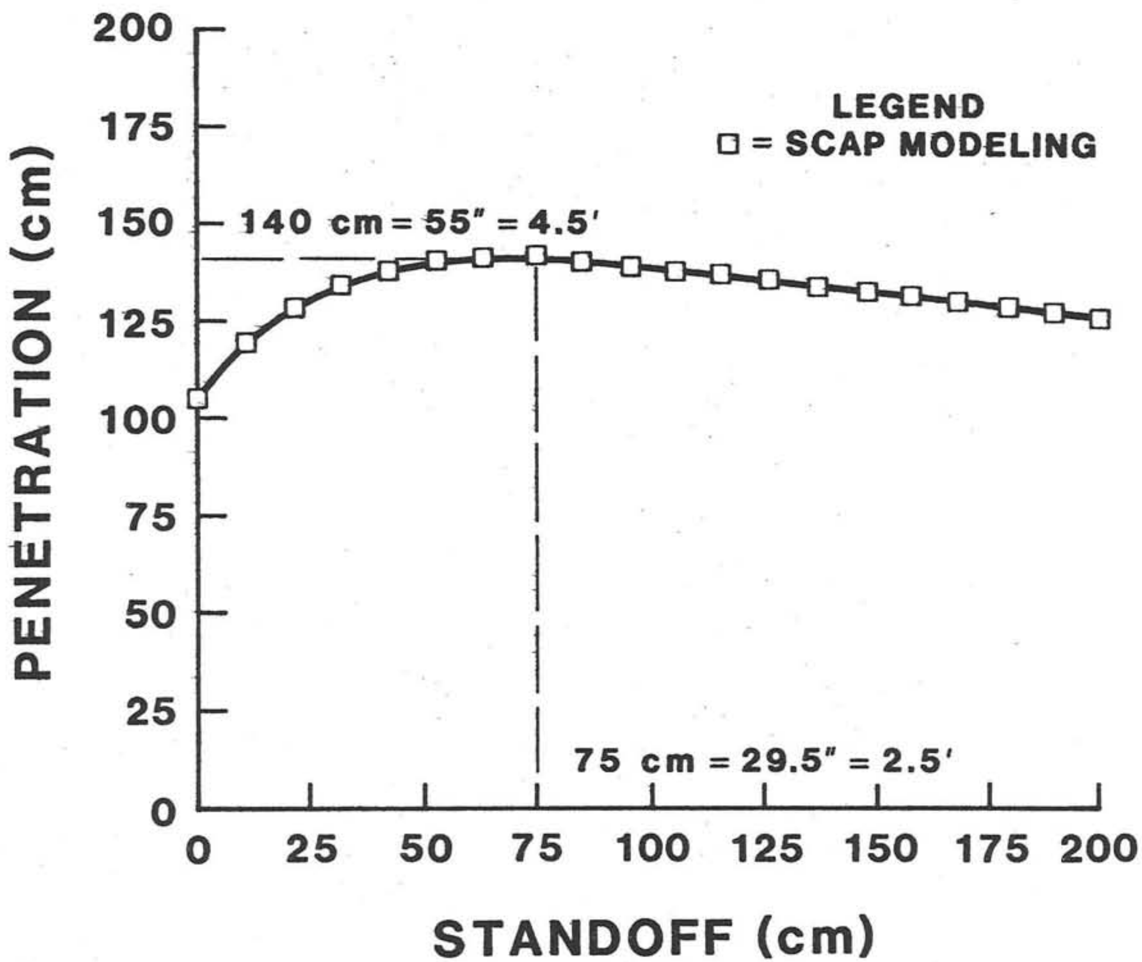

Figure 23. 4.66 CSC Jet Penetration Versus Standoff for a Tuff Target

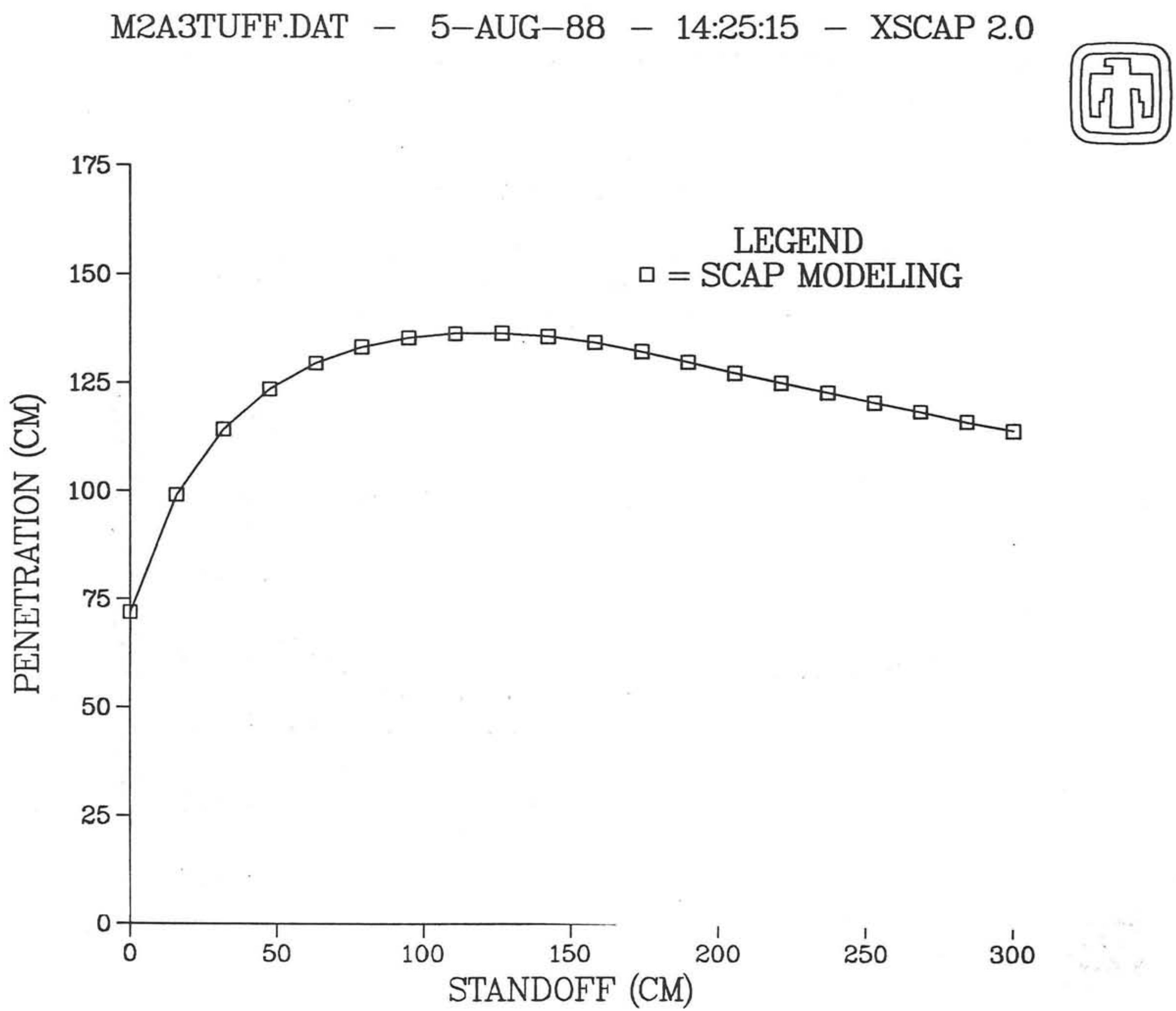

Figure 24. 6.986 Inch Diameter M2A3 CSC Penetration Versus Standoff

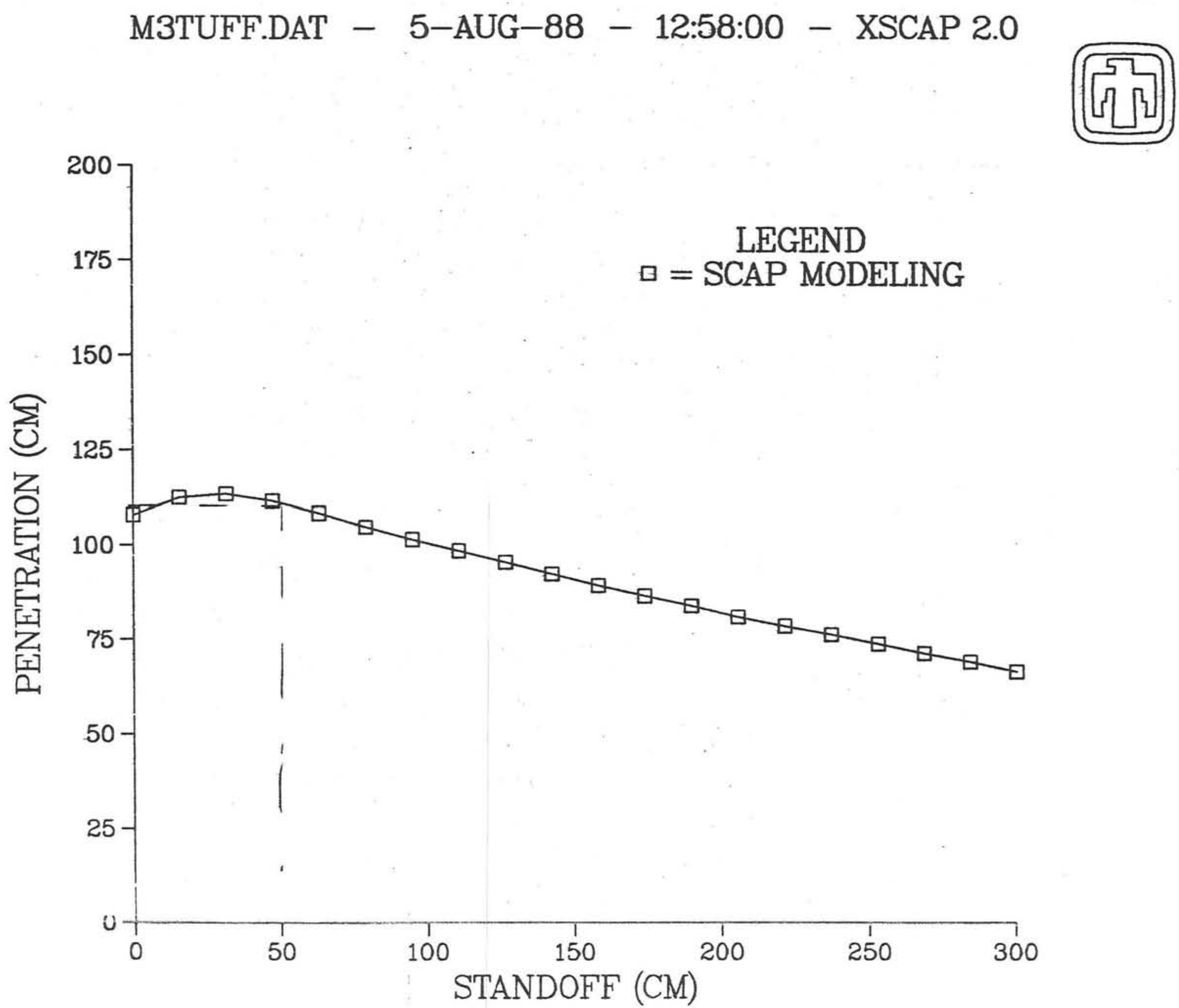

Figure 25. 9.125 Inch Diameter M3 CSC

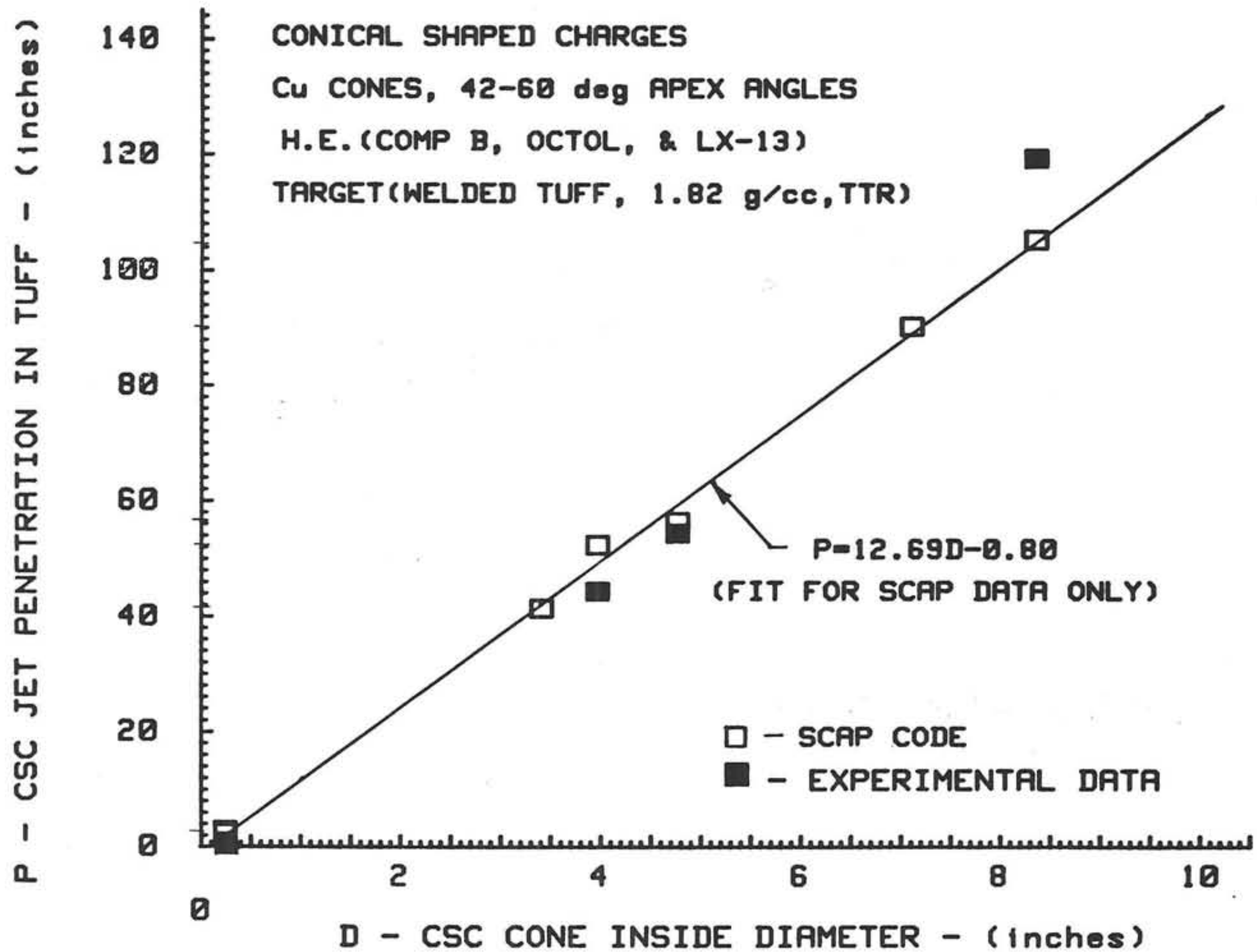

FIGURE 26. CONICAL SHAPED CHARGE JET PENETRATION INTO WELDED TUFF FORMATIONS AT TONAPAH TEST RANGE

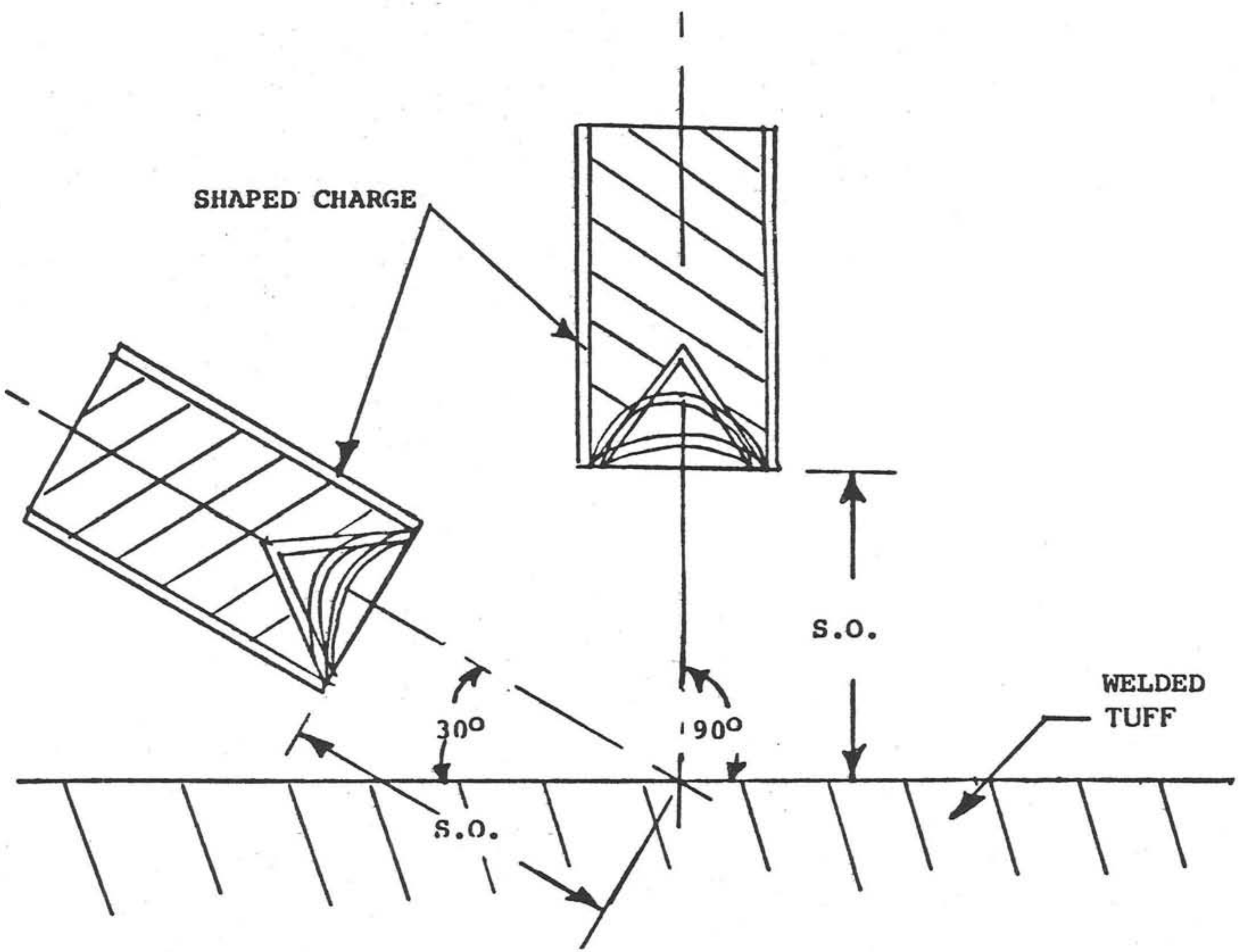

Figure 27. Shaped Charge Orientations Relative to Tuff Formation Surface

Figure 28. 3.86 Inch Diameter CSC Test Configuration

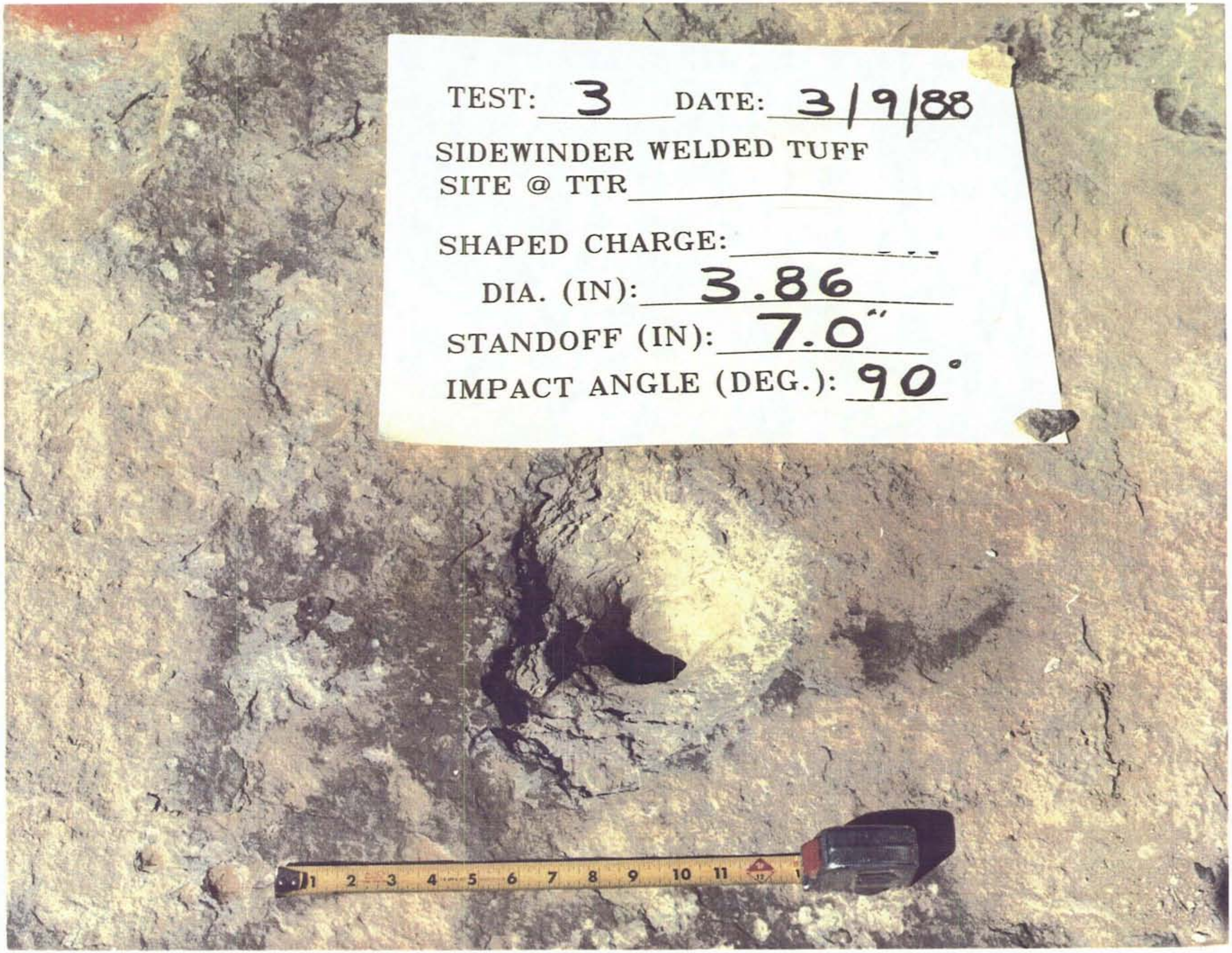

Figure 29. 3.86 Inch Diameter CSC Generated Hole in Tuff

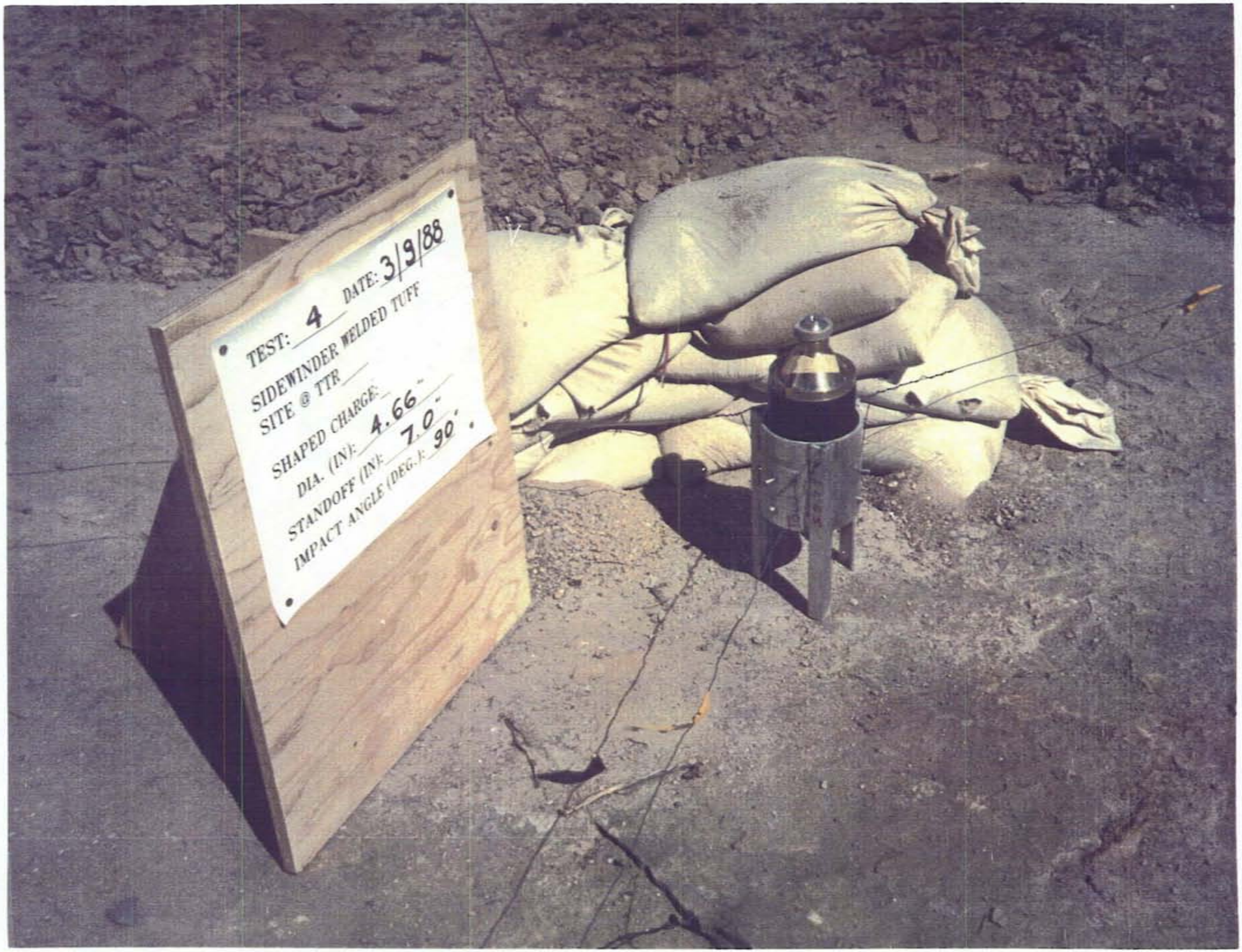

Figure 30. 4.66 Inch Diameter CSC Test Configuration

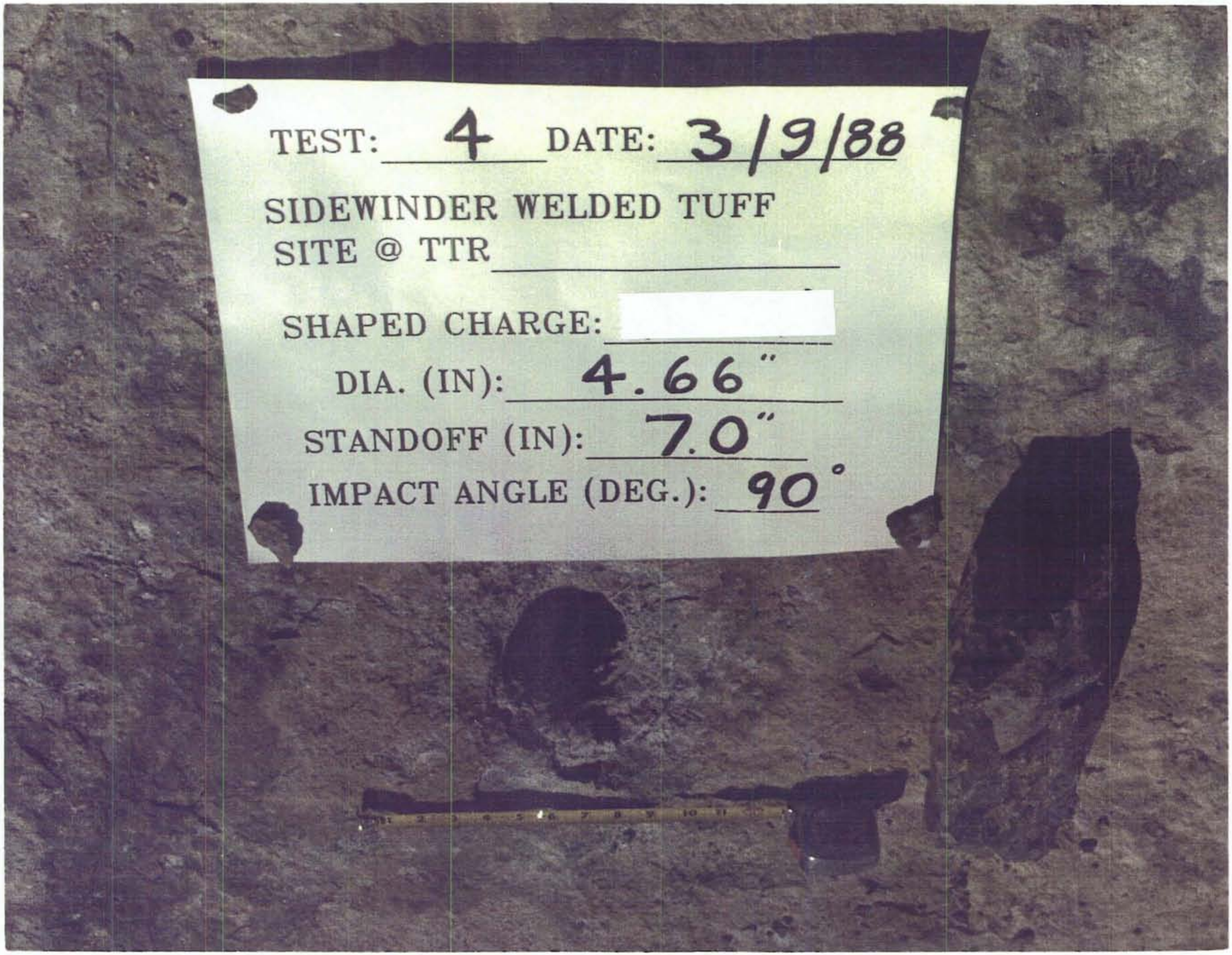

Figure 31. 4.66 Inch Diameter CSC Generated Hole in Tuff

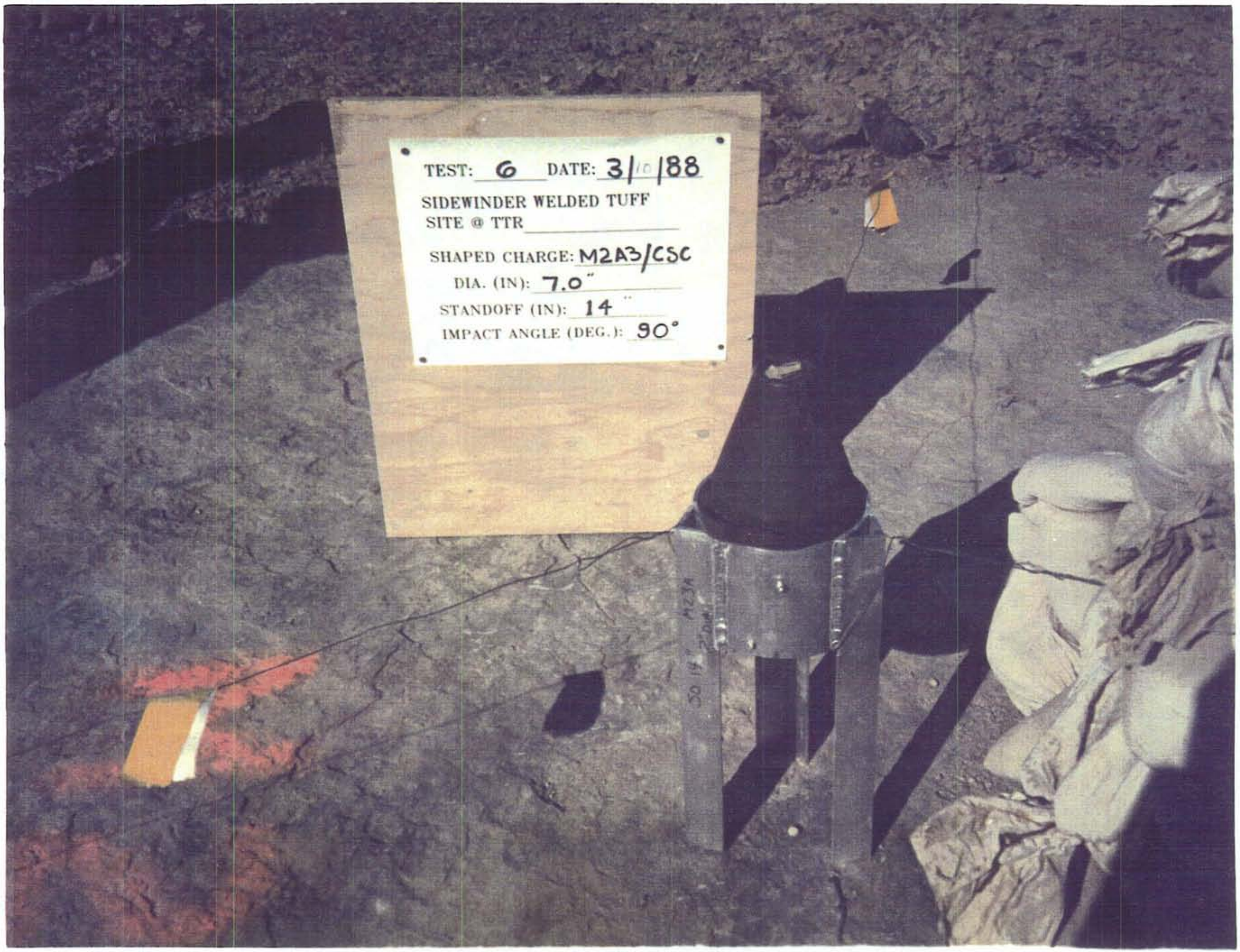

Figure 32. 7.0 Inch Diameter CSC Test Configuration

Figure 33. 7.0 Inch Diameter CSC Generated Hole in Tuff

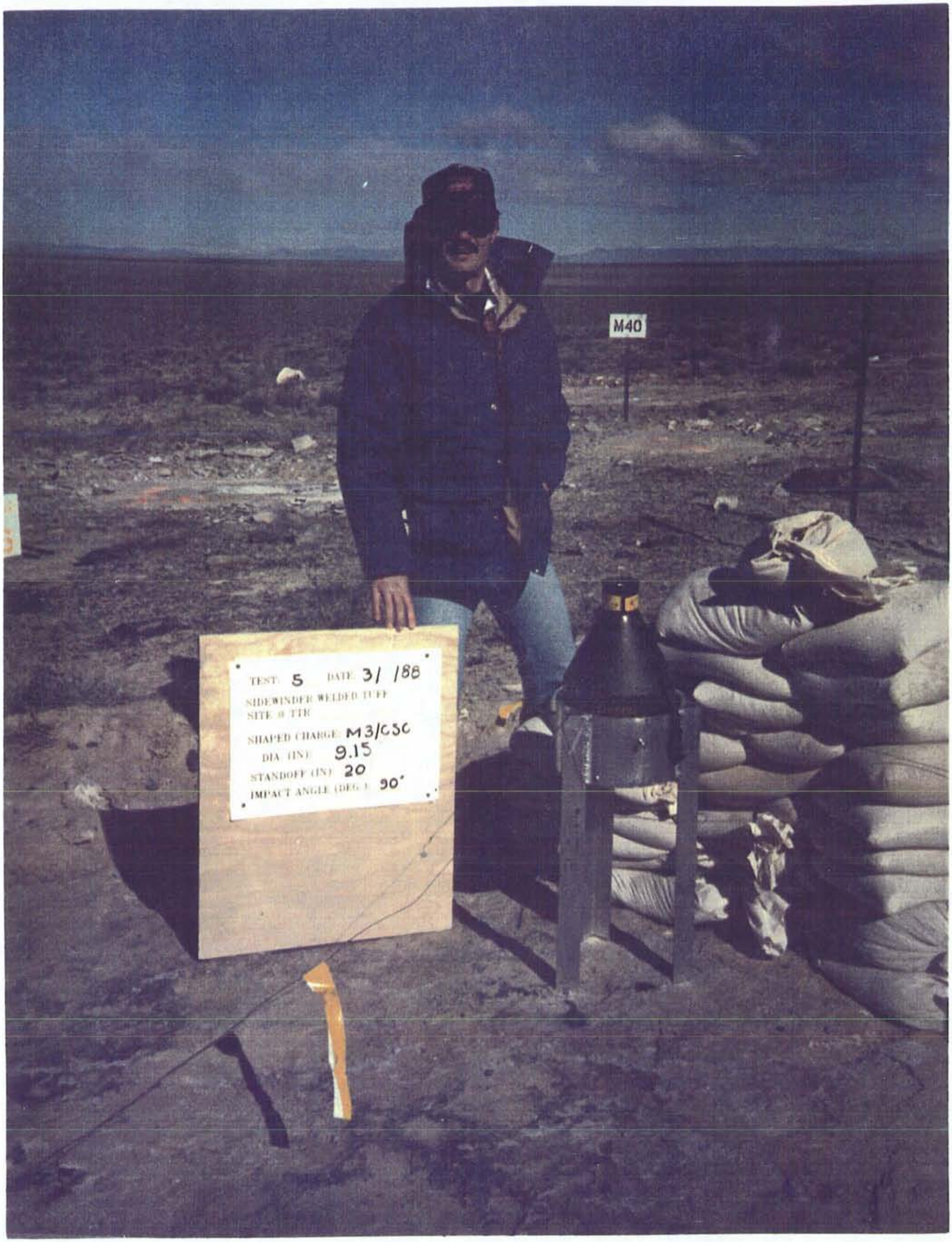

Figure 34. 9.125 Inch Diameter CSC Test Configuration

Figure 35. 9.125 Inch Diameter CSC Generated Hole in Tuff

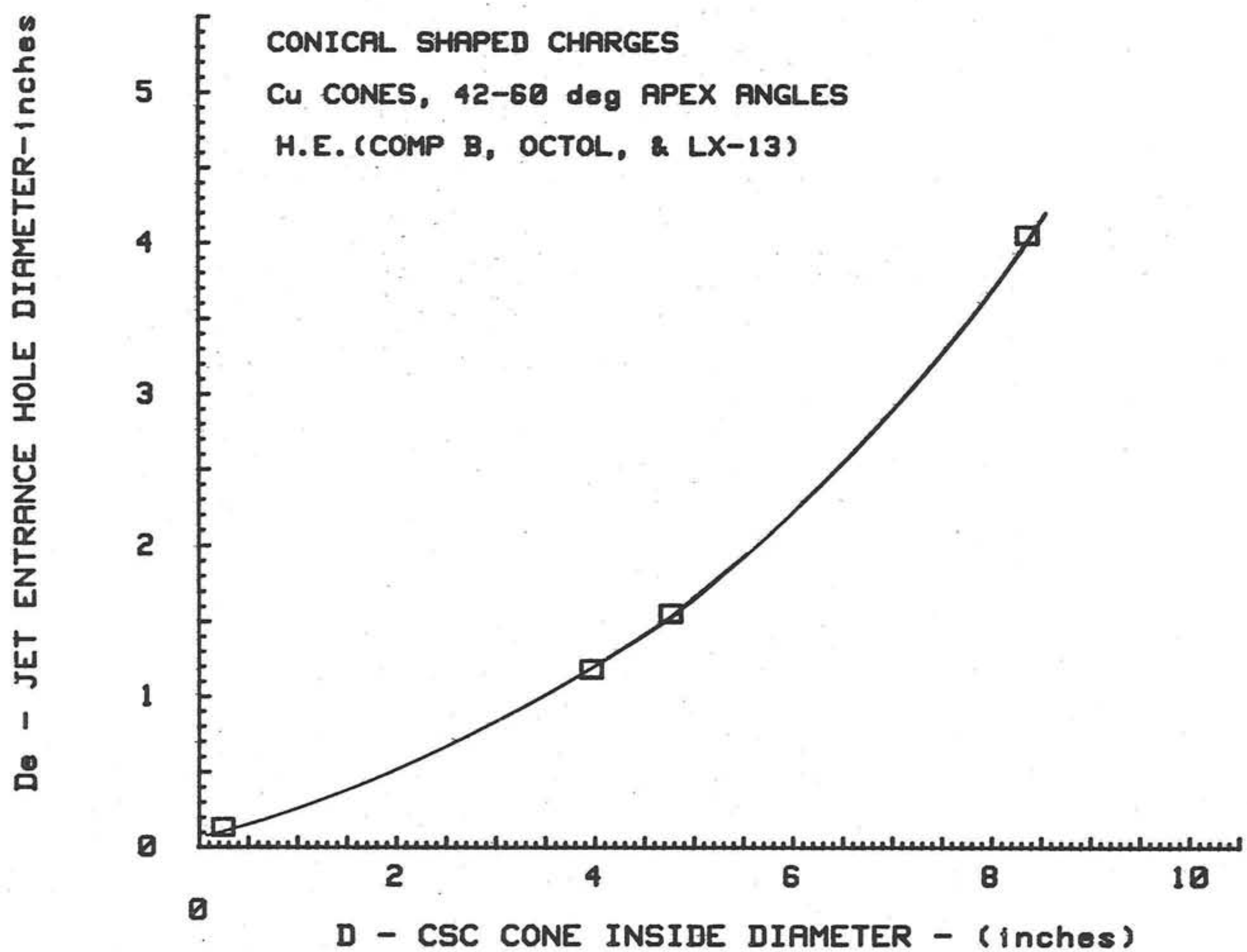

FIGURE 36. CONICAL SHAPED CHARGE JET ENTRANCE HOLE DIAMETER IN TUFF AS A FUNCTION OF CSC CONE INSIDE DIAMETER

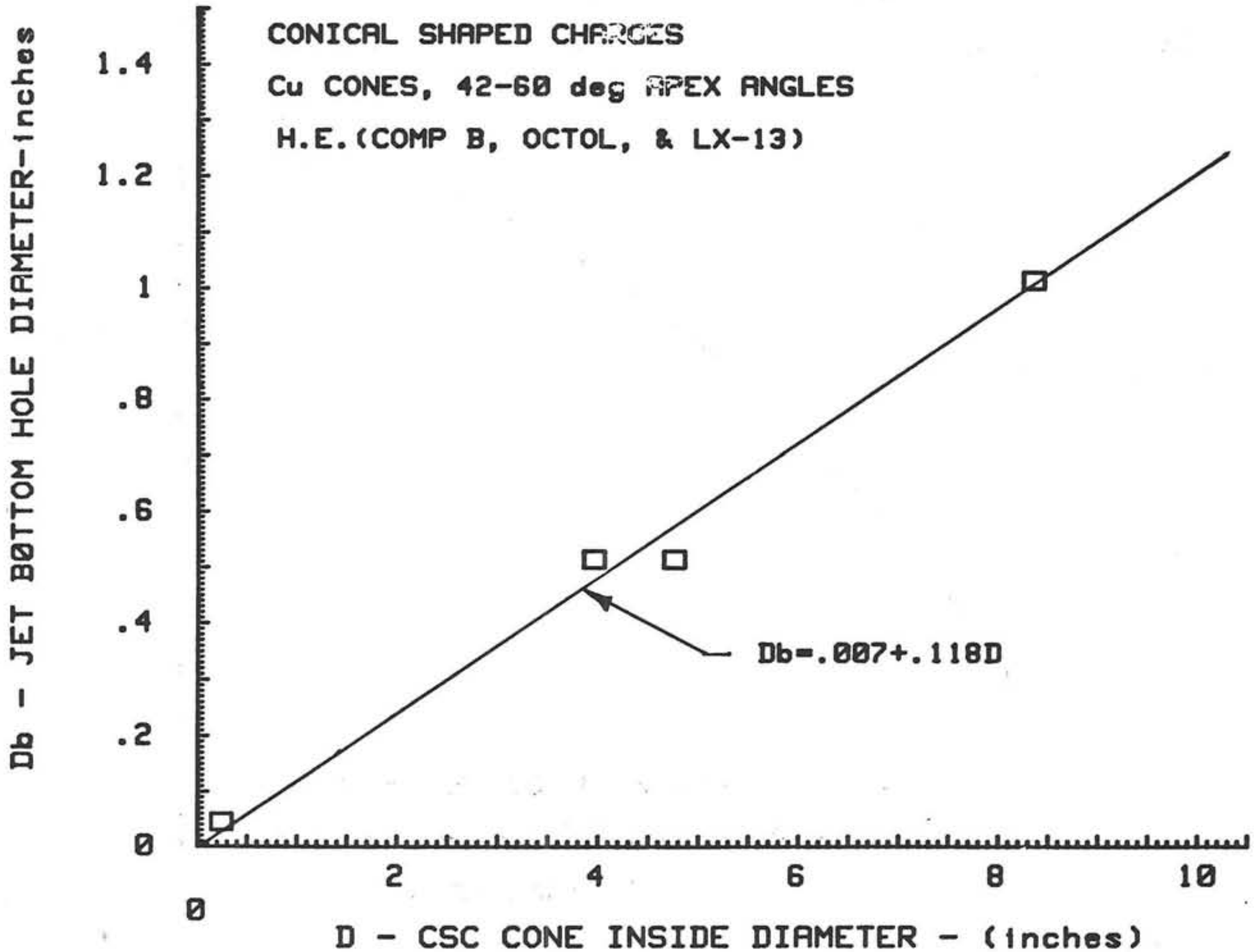

FIGURE 37. CONICAL SHAPED CHARGE JET BOTTOM HOLE DIAMETER IN TUFF AS A FUNCTION OF CSC CONE INSIDE DIAMETER

EXPLOSIVE FORMED PROJECTILE CONFIGURATION

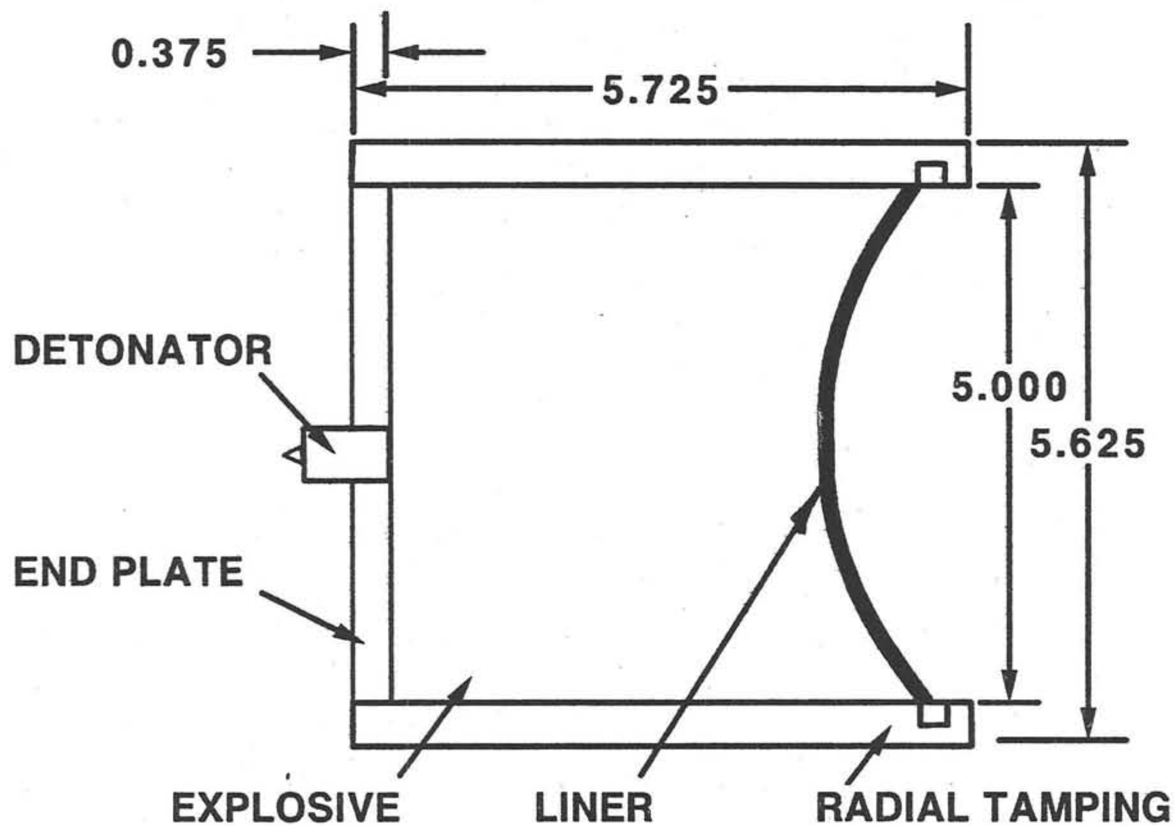

Figure 38.

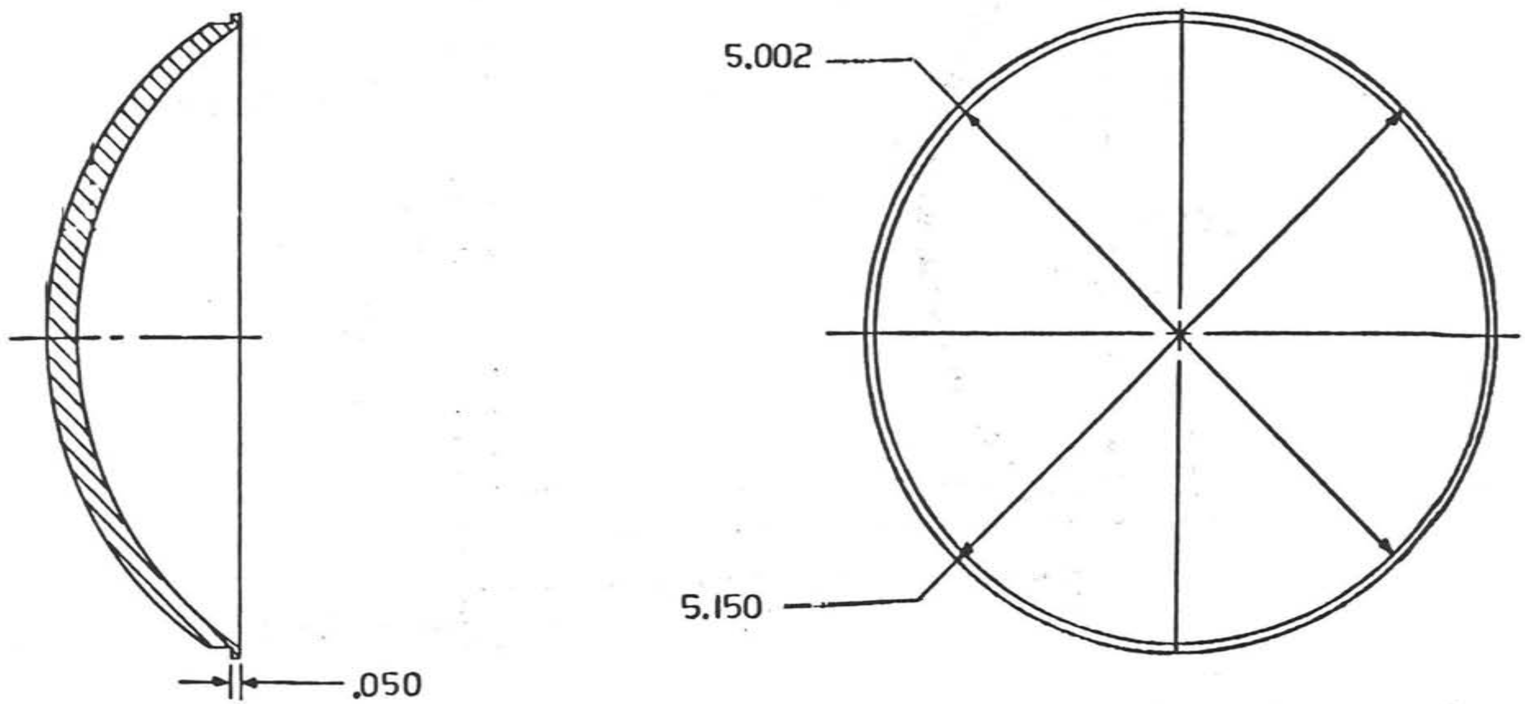

Figure 39. EFP Copper Liner for 5.0 Inch Inside Diameter EFP

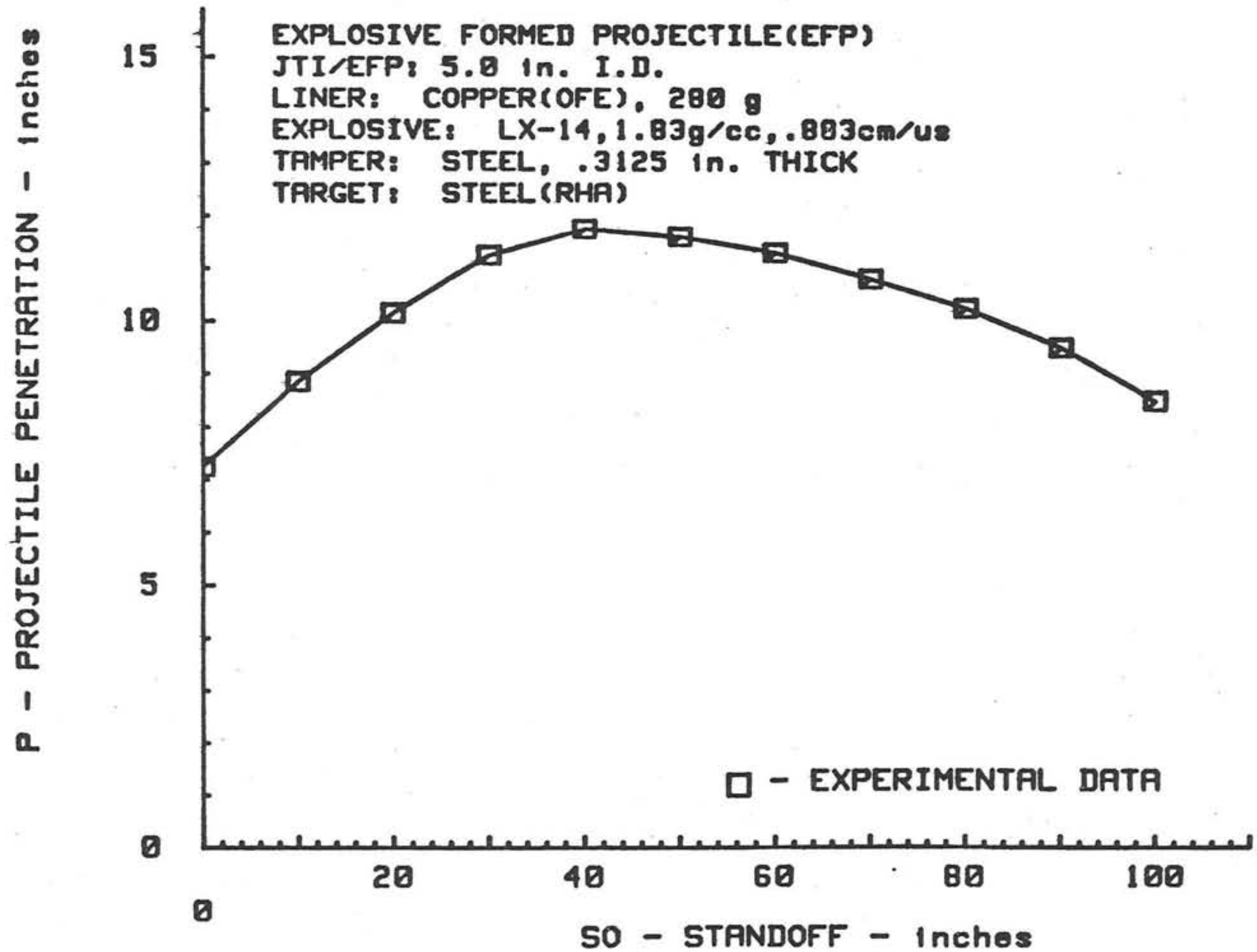

FIGURE 40. JTI EXPLOSIVE FORMED PROJECTILE MEASURED PENETRATION INTO STEEL(RHA) TARGET VERSUS STANDOFF

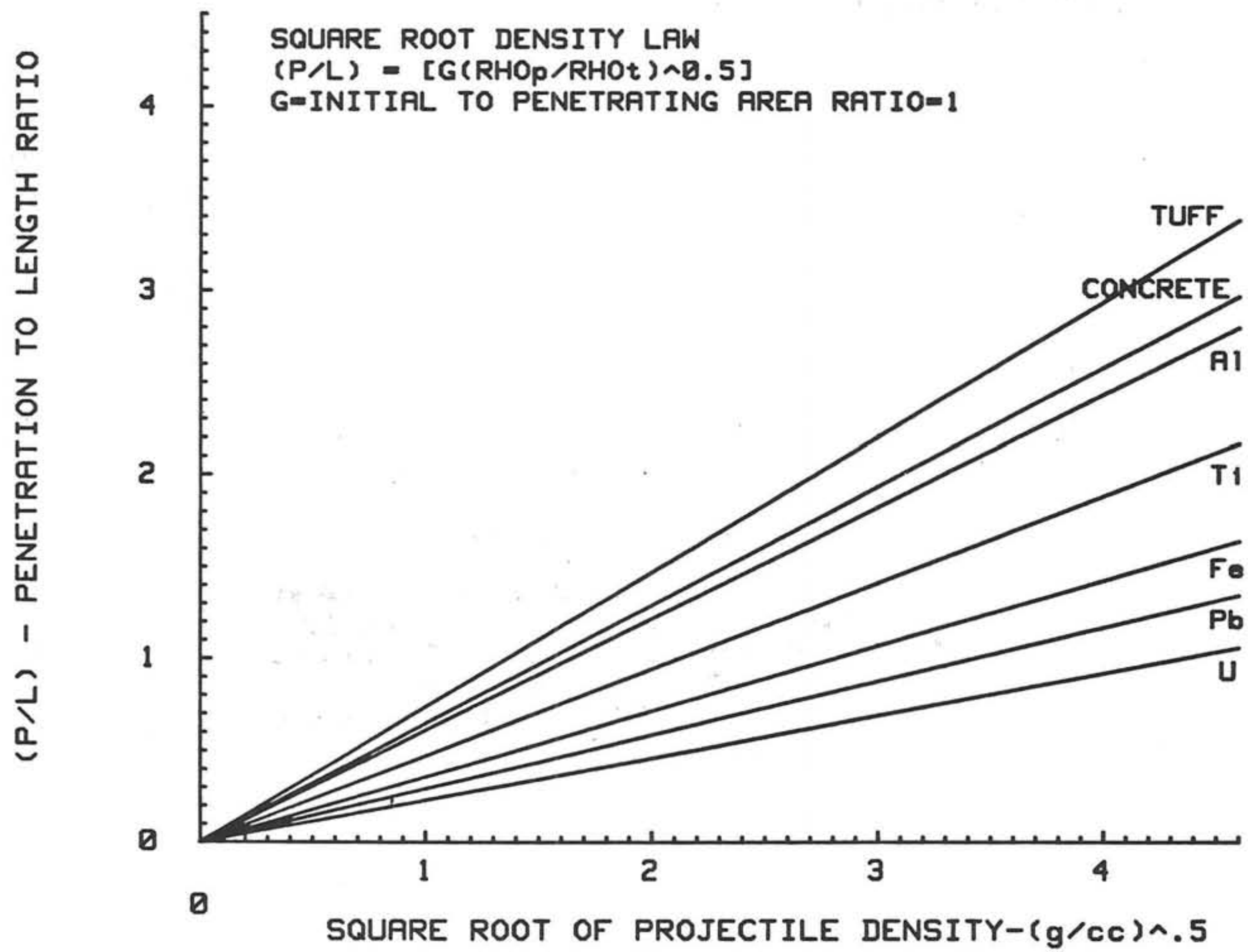

FIGURE 41. PROJECTILE PENETRATION TO LENGTH RATIO VERSUS SQUARE ROOT OF PROJECTILE DENSITY AND TARGET

Figure 42. EFP Test Configuration for 90 Degree Impact of Tuff Target

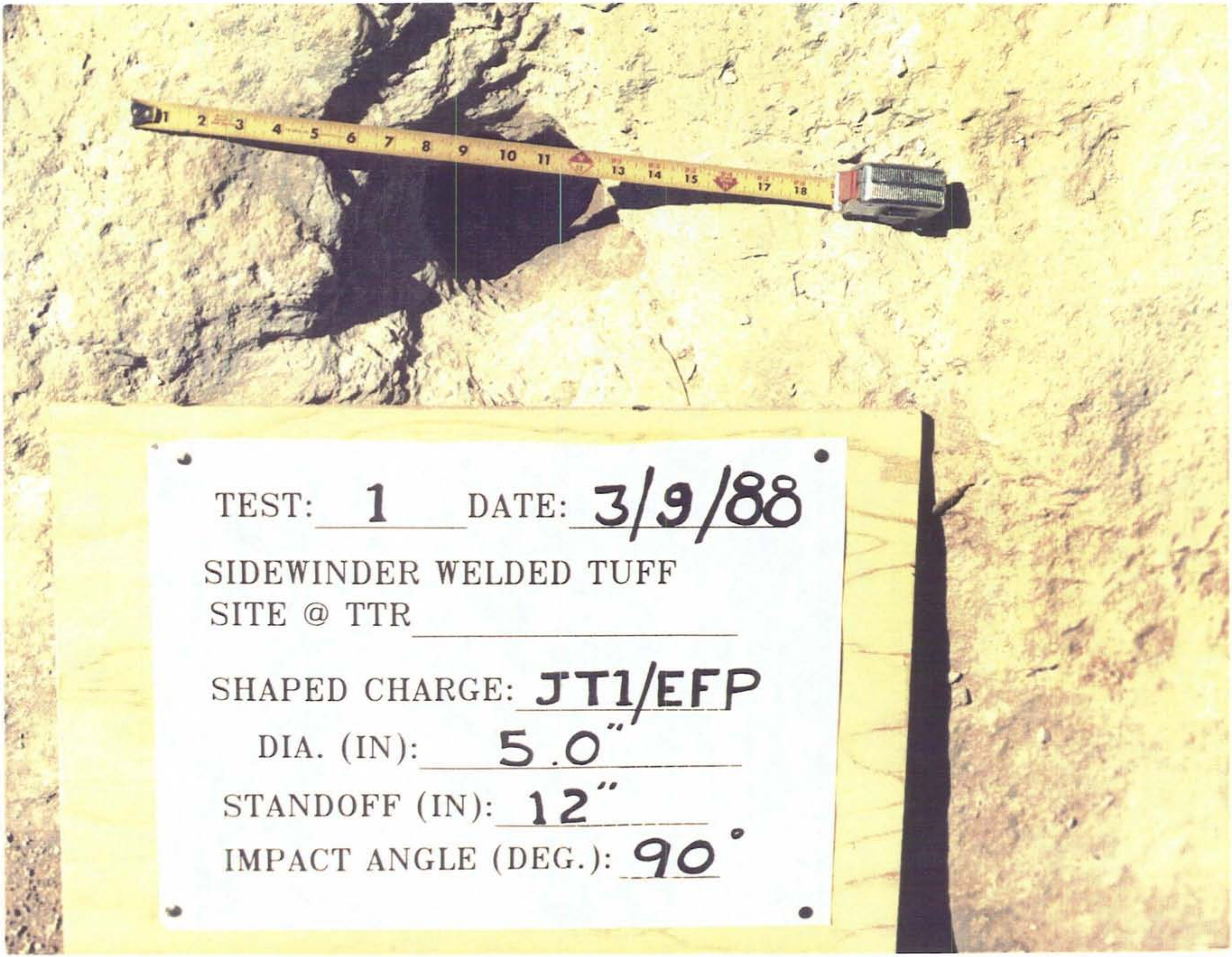

Figure 43. EFP Slug Generated Hole in Tuff Target

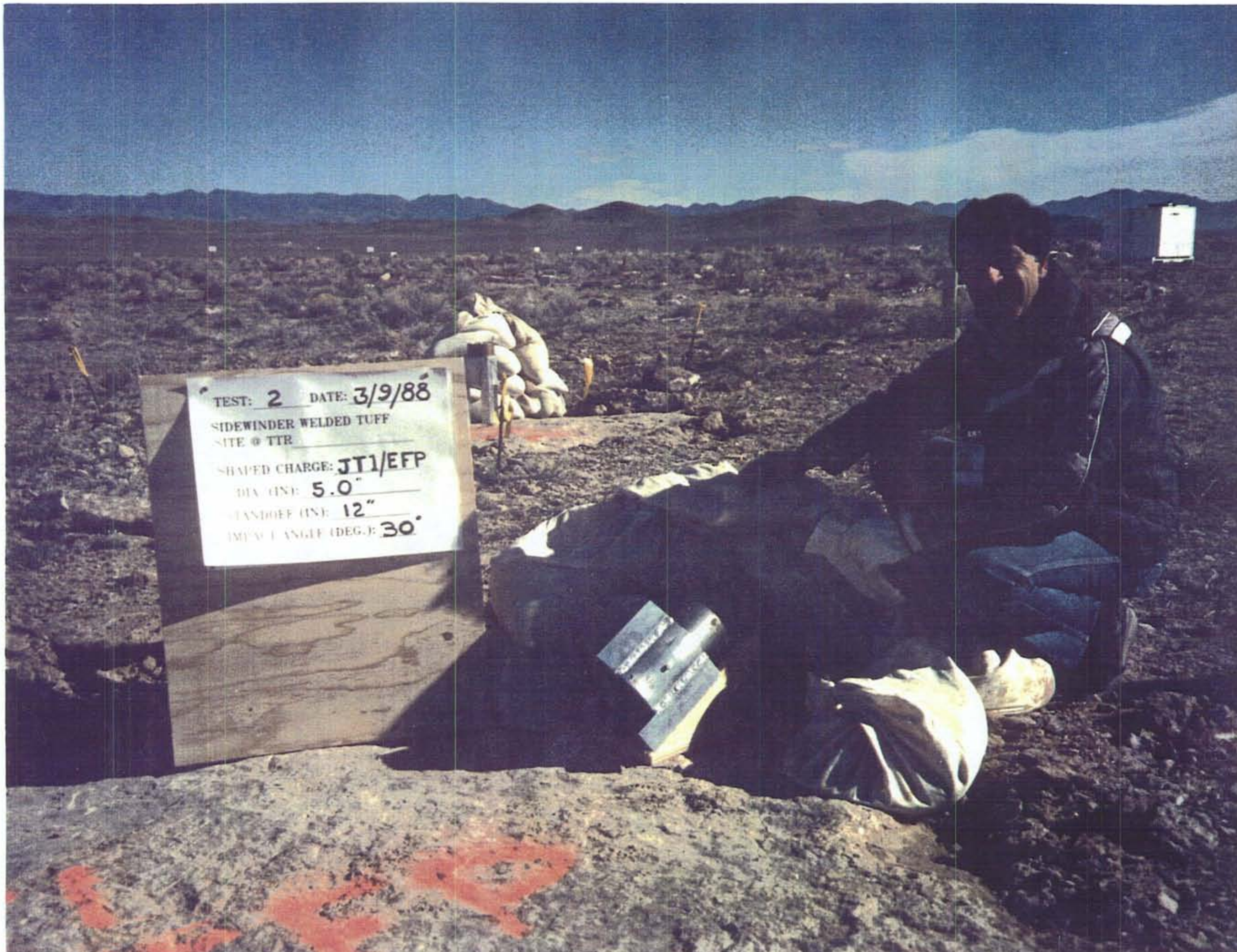

Figure 44. EFP Test Configuration for 30 Degree Impact of Tuff Target

Figure 45. EFP Slug Generated Hole in Tuff Target

Distribution:

Aerojet Ordnance Co.
Attn: J. Carleone
2521 Michelle
Tustin, CA 92680

Ballistic Research Lab (10)
Aberdeen Proving Ground
Attn: D. Dietrich
R. J. Eichelberger
F. Grace
J. T. Harrison
R. Jameson
K. Kimsey
M. Lampson
S. B. Segletes
W. P. Walter
S. K. Golaskie
Aberdeen, MD 21005

Joseph Backofen
P. O. Box 1925
Washington, DC 20013

Battelle Columbus Laboratory (2)
Attn: J. White
D. R. Trott
505 King Avenue
Columbus, OH 43201

Ctr for Explosives Tech. Research
New Mexico Technical Institute
Attn: Per-Anders Persson
Socorro, NM 87801

Dyna East Corp (3)
Attn: P. C. Chou
R. C. Ciccarelli
W. J. Flis
3132 Market Street
Philadelphia, PA 19104

Honeywell, Inc. (2)
Defense Systems Group
Attn: J. Houlton
G. R. Johnson
10400 Yellow Circle Drive
Minnetouba, MN 55343

Lawrence Livermore National Lab (6)
Attn: M. Finger
J. D. Immele
J. L. Levatin
M. J. Murphy
M. Van Thiel
M. L. Wilkins
P. O. Box 808
Livermore, CA 94550

Los Alamos National Lab (12)
Attn: J. D. Allen, G787
R. Carver, B265
E. H. Farnum, G756
M. Ginsberg, J960
L. W. Hantel, F668
J. Hopson, F664
R. Karpp, P940
J. Repa, J960
P. Studt, F668
R. J. Young, F664
J. M. Walsh, P940
R. McCormick, P950
P. O. Box 1663
Los Alamos, NM 87545

Naval Weapons Center
Materials Eng. Branch
Attn: G. A. Hayes
China Lake, CA 93555

Teledyne (3)
Attn: B. Heideman
D. F. Elliott
W. B. Richardson
3601 Union Road
Hollister, CA 95023

U.S. Army Armament Research
and Development Center
Attn: A. Garcia
Building 354
Dover, NJ 07801

E. I. DuPont de Nemours & Co, Inc.
Attn: F. C. Sawyers
3520 Pebble Beach Dr
Farmers Branch, TX 75234

Explosive Technology (2)
Attn: M. D. Anderson
J. E. Kennedy
P. O. Box KK
Fairfield, CA 94533-0659

Mason & Hanger (6)
Silas Mason Co., Inc
Pantex Plant
Attn: D. Garrett
R. Slape
D. Hilleary
D. Schaffer
P. Kramer
C. A. Campos
P. O. Box 30020
Amarillo, TX 79177

Allied-Signal Aerospace Co
Kansas City Div.
Attn: G. Oswald
P. O. Box 1159
Kansas City, MO 64141

Unidynamics/Phoenix, Inc. (2)
Attn: R. Smith
J. Fronabarger
P. O. Box 2990
Phoenix, AZ 85062

Ensign-Bickford Co (4)
Aerospace Division
Attn: L. Mecca
B. Boggs
K. Puls
E. Tarca
660 Hopmeadow St.
Simsbury, CT 06070

Jet Research Center, Inc.
P. O. Box 246
Arlington, TX 76010

Lockheed Missiles & Space Co (5)
Attn: W. E. Moffatt
R. Weinheimer
J. Meeks
J. P. Beck
N. Markovich-Cottong
1111 Lockheed Way
Sunnyvale, CA 94086

Southwest Research Institute
Attn: A. B. Wenzel
6220 Culebra Road
PO Drawer 28510
San Antonio, TX 78284

Strategic Systems Project Office
Department of the Navy
Attn: D. Kenemuth, 27314
Washington, DC 20376

Distribution:

1131	B. Morosin
1413	G. G. Weigand
1500	W. Herrmann
1510	J. W. Nunziato
1512	J. C. Cummings
1513	D. W. Larsen
1521	R. D. Krieg
1522	R. C. Reuter
1523	J. H. Biffle
1524	D. B. Longscope
1530	L. W. Davison
1533	P. Yarrington
1533	M. E. Kipp
1533	A. C. Robinson
2500	D. B. Hayes, Actg
2510	D. H. Anderson
2512	J. G. Harlan
2512	D. R. Begeal
2512	S. G. Hallett
2512	R. G. Jungst
2512	D. L. Marchi
2512	M. G. Vigil (15)
2513	D. E. Mitchell
2513	S. G. Barnhart
2513	T. L. Garcia
2514	P. L. Stanton
2514	L. L.Bonzon
2515	P. D. Wilcox
2515	M. R. Kopczewski
2515	V. M. Loyola
2542	W. N. Sullivan
2600	L. D. Bertholf
3141	S. A. Landenberger (5)
3151	W. I. Klein (3)
3141-1	C. L. Ward (8) For DOE/OSTI
5120	W. R. Reynolds
5121	D. F. McVey
5121	O. R. Berg
5121	D. L. DeWerff
5121	M. M. Plugge
5128	B. E. Bader
5128	K. E. Mead
5165	S. D. Meyer
5165	R. K. Thomas
5165	N. R. Hansen
5165	W. J. Errickson
5165	W. J. Patterson
5165	L. B. Traylor
5251	T. A. Sellers, Actg
5251	L. A. Suber
5262	J. W. Kane
6230	W. C. Luth
6320	J. E. Stiegler
6321	R. E. Luna
6321	R. P. Sandoval
6322	J. M. Freedman
6323	G. C. Allen
6323	H. R. Yoshimura
6400	D. J. McCloskey
6416	R. M. Cranwell
6416	E. L. Emerson
6416	J. S. Philbin
7130	J. D. Kennedy
7133	O. L. Burchett
7133	P. W. Cooper
7133	S. R. Kurowski
7170	R. D. Bentley
7173	G. L. West
7173	H. D. Smith
7533	F. H. Mathews
7533	J. P. Weber
7535	D. C. Bickel
8524	P. W. Dean